농학박사학위논문

Metabolic Profiles of Grapevines Infected with *Pseudocercospora vitis* and *Agrobacterium vitis*

포도나무 갈색무늬병과 줄기혹병에 감염된 포도나무의 대사물질 유형

2017년 2월

서울대학교 대학원

농생명공학부 식물미생물학전공

정 성 민

A THESIS FOR THE DEGREE OF DOCTOR OF PHILOSOPHY

Metabolic Profiles of Grapevines Infected with *Pseudocercospora vitis* and *Agrobacterium vitis*

BY
SUNG MIN JUNG

Department of Agricultural Biotechnology

The Graduate School of Seoul National University

February 2017

농학박사학위논문

포도나무 갈색무늬병과 줄기혹병에 감염된 포도나무의 대사물질 유형

지도교수 김 영 호

이 논문을 농학박사학위논문으로 제출함

2016년 10월

서울대학교 대학원 농생명공학부 식물미생물학전공

정 성 민

정성민의 박사학위논문을 인준함

2016년 12월

위 원 장 _____ (인)

부 위 원 장 _____ (인)

위 원 _____ (인)

위 원 _____ (인)

위 원 _____ (인)

A THESIS FOR THE DEGREE OF DOCTOR OF PHILOSOPHY

Metabolic Profiles of Grapevines Infected with *Pseudocercospora vitis* and *Agrobacterium vitis*

UNDER THE DIRECTION OF DR. YOUNG HO KIM

SUBMITTED TO THE FACULTY OF THE GRADUATE SCHOOL OF
SEOUL NATIONAL UNIVERSITY
BY SUNG MIN JUNG

MAJOR IN PLANT MICROBIOLOGY
DEPARTMENT OF AGRICULTURAL BIOTECHNOLOGY

February 2017

APPROVED AS A QUALIFIED THESIS OF SUNG MIN JUNG
FOR THE DOCTOR OF PHILOSOPHY
BY THE COMMITTEE MEMBERS

C H I A R M A N _____

VICE CHIARMAN _____

M E M B E R _____

M E M B E R _____

M E M B E R _____

ABSTRACT

Metabolic Profiles of Grapevines Infected with *Pseudocercospora vitis* and *Agrobacterium vitis*

SUNG MIN JUNG
Major in Plant Microbiology
Department of Agricultural Biotechnology
The Graduate School of Seoul National University

In this study, profilings of disease-related metabolites were assessed for characterizing two major grapevine diseases, leaf spot caused by *Pseudocercospora vitis* and crown gall caused by *Agrobacterium vitis*, respectively, for both of which GC-MS and multivariate data analysis were applied as the analytical instrumentation and statistical validation. For the leaf spot, a total of 20 metabolites were determined to have their relations with lesion symptoms and the periphery of the leaf spot symptoms, most of which were increased in their contents in the periphery of the symptoms compared with the necrotic lesions. For the crown gall, 13 metabolites increased significantly in relation to the response types, mostly at post-inoculation stages, more prevalently (8 metabolites) at two days after inoculation than other stages, and more related to the susceptible response type (SS) (7 metabolites) than resistant (RR) (3 metabolites) or

moderately resistant (SR) (one metabolite) response type. This suggests that most of the disease-related metabolites may be induced by the pathogen infection largely for facilitating gall development except resveratrol, a phytoalexin involved in the resistance response (RR). A total of six metabolites were identified from the comparison of the metabolite profiling between the leaf tissues with and without leaf spot symptoms, including maltotriose, glucoheptonic acid and tartronic acid, a phenolic compound 1-hydroxyanthraquinone and two amino acids aspartic acid and L-threonine. This suggests these may be the disease-related metabolites occurring widely around the infection sites of the leaf tissues with the leaf spot. For the crown gall, most numerous metabolites related to the infection or wound significantly occurred at 2 days after inoculation (DAI) (post-1) (8 for infection in SS, 4 for wound in RR), second-most at 7 DAI (post-2) (3 for infection in SS, 6 and 1 for wounding in SS and RR, respectively), and least at 30 DAI (post-3) (all 3 for infection in RR or SR), suggesting that the responses to the pathogen infection mostly occur in the susceptible grapevines at post-1, and those to wounding (wound healing) occur earlier in the grapevines with RR than those with SS or SR. It also suggests the responses to wounding should be completed and no more wound-related metabolites are detected at post-3. All of the results suggest that plant resistance and wound healing responses are inter-related, enhancing the other responses to increase resistance to the pathogen infection and to speed up the wound healing processes. These disease characteristics revealed by metabolite profiling would provide valuable information and new insights on the understandings of the diseases so as to be used for the development of grapevine disease management strategies.

KEYWORDS: *Agrobacterium vitis,* metabolites profiling, *Pseudocercospora vitis,* response type, wounding

Student Number : 2006-30889

CONTENTS

page

LIST OF TABLES

LIST OF FIGURES

ABBREVIATIONS

CV-ANOVA : Cross-validated analysis of variance;

FAME : Fatty Acid Methyl Ester;

MSTFA : N-methyl-N-(trimethylsilyl)-trifluoroacetamide;

OPLS-DA : Orthogonal projections to latent structures discriminant analysis;

PCA : Principal component analysis;

PLS : Partial Least Squares;

VIP : Variable importance for projection

GENERAL INTRODUCTION

Grapevine

Grapes are one of the world's most planted fruits with a high value. Currently, the grapes are cultivated in 7.5 million ha with the total annual production of 74 million tons worldwide (OIV annual report, 2015). Cultivation of the grapevine by humans began during the Neolithic era (BC 6000 ~ 5000) along the eastern shores of the Black Sea (Mullins et al., 1992). The genus *Vitis* contains about 60 species, of which about 40 species are native to North America and about 20 species are native to central or eastern Asia (Aradhya et al., 2003). There are 24,000 named cultivars, but most of them are synonyms. The number of the different and distinguishable cultivars is about 5,000 (Creasy and Creasy, 2009). European grape (*V. vinifera*) is susceptible to a variety of diseases unless grapevine planted in Mediterean climate. However, most of the northern American species are resistant to most grape diseases. So many brand-new cultivars have been developed by cross breeding interspecific cultivars (*V. vinifera* x *V. labluscana*) for overcoming unfavorable environments (Yamada and Sato, 2016).

Fungal and Bacterial Diseases in Grapevine

In the middle of the eighteen century, some of the northern American fungal pathogens were transferred to European vineyards. Powdery mildew (*Erysiphe necator*), downy mildew (*Plasmopara viticola*), and black rot (*Guignardia bidwellii*) had seriously adverse influences on

the grape quality and production yield (Wilcox et al., 2015). There are three bacterial and 34 fungal (or pseudo fungal) diseases in the grapevine (Wilcox et al., 2015), among which several fungal diseases destroy the whole vineyard within a short period of grapevine growing season without fungicidal sprays. Downy mildew, powdery mildew, and ripe rot not only damage severely grape quality and yield but also reduce grapevine tree vigor in the following year. In Korean vineyard, the major diseases are one fungal disease, brown leaf spot caused by *Pseudocercospora vitis* (Kim and Shin, 1998) and another bacterial disease, crown gall, caused by *Agrobacterium vitis* (Ophel and Kerr, 1990), which exert significantly critical damages to Korean vineyard every year.

Leaf spot disease caused by *Pseudocercospora vitis*

Grapevine leaf spot is caused by *Pseudocercospora vitis* Speg. in Korea (Kim and Shin, 1998), which is called leaf blight in American (Wilcox et al., 2015). In many cases of severe brown spot disease, soluble solids of grape decrease by 20% (Park et al., 2004). Fruiting structures of this fungus are black synnemata (200~500 um) that bear brown, elongate, 3~17 septated conidia (25~99 x 4~8 um) (Wilcox et al., 2015). Leaf spot disease rarely occurs in the Mediterranean climate, but reportedly often occurs in tropical and subtropical humid areas of the world (Dang and Daulta, 1982; Liang et al., 2016; Sisterna and Ronco, 2005). The grape cultivar 'Campbell Early' planted in about 70% of Korean vineyards is susceptible to leaf spot disease caused by *P. vitis* (Kim and Shin, 1998). Leaf spot disease often causes early defoliation of the grapevine that

can be led to severely decreased grape quality and vine vigor in the following year (Jung et al., 2009; Liang et al., 2016; Park et al., 2006). The leaf spot disease cycle initiates from overwintered conidia on the leaves fallen in the previous year that spread with the wind on the new grapevine leaves, where they germinate at a relative humidity of 80%. When minimum temperature during the day reaches above 20℃, leaf spot disease starts destructive epidemics, showing the conidial germination of about 60% at 25℃without light (Jung et al., 2009; Maia et al., 2015). In Korea, the leaf spot disease is very difficult to control by fungicidal spray because the disease occurs prevalently in the same period with the rainy season when it is too close to grape harvest time to spray chemicals. Little study has been conducted on the chemical control of the grapevine leaf spot because this disease is of little importance in major grape-producing areas in the world.

Crown gall disease caused by *Agrobacterium vitis*

Crown gall of grapevine reduces the grape yield by 20~40% and trunk diameter approximately by 9%, compared to healthy uninfected grapevines (Schroth, 1988). Crown gall disease is one of the difficult diseases to control by chemicals in vineyards. The causal agent of grapevine crown gall, *Agrobacterium vitis*, is a different biovar from other *Agrobacterium* spp. because it can induce a grapevine-specific crown gall (Ophel and Kerr, 1990; Panagopoulos and Psallidas, 1973). Crown gall disease initiates by invading grapevine root with the necrotic lesion, followed by the transfer of the T-DNA from the pathogen (*A. vitis*) in type 4 secretion system into the

plant cell (Low et al., 2014). T-DNA contains genes for biosynthesis of auxins (*iaaM* and *iaaH*) and cytokinins (*ipt* genes) (Burr and Otten, 1999), resulting in the increase of the plant hormone contents in vascular cambium, leading to uncontrolled growth of gall tissues that produce special compounds (opine) for nourishing the pathogen (Wilcox et al., 2015). *A. vitis* have a special gene for living on grapevine tissue, dehydrogenase (*ttuC* gene) of tartrate, which is abundant organic acid in the grapevine, providing competitive advantages to *A. vitis* (Burr and Otten, 1999). Another host-specific gene is polygalacturonase (PG) gene (*pehA* gene) that facilitates *A. vitis* attachment and colonization on the grapevine. Two different strategies were tried to control crown gall disease; use of the rootstock cultivars, 3309C, 5BB, 101-14 MGT and Gloire, resistance to crown gall disease (Ferreira and van Zyl, 1986; Süle and Burr, 1998) and use of avirulent nontumorigenic *A. vitis*, F2/5 that antibiotically inhibits crown gall development (Burr et al., 1997).

Metabolomics and multivariate analysis

Metabolic profiling is the measurement of hundreds or potentially thousands of metabolites. It requires a streamlined pipeline for extraction, separation, and analysis (Kopka et al., 2004). Metabolomics starts from functional genomic analyses which emphasize analyses at the level of gene expression (transcriptomics), translation (proteomics), and their product (metabolomics), which are approached with the idea of defining the phenotype and finally bridging the genotype to phenotype gap (Goodacre, 2005). In *Arabidopsis*, profound phenotypes information has been

connected to their genomics data (Fiehn et al., 2000), whose approaches have helped to understand gene function between some random mutant lines and phenotype of metabolic disorders. Metabolite profiling is focused on an analytical procedure that can be restricted to the identification and quantification of a selected number of pre-defined metabolites in a biological sample (Fiehn, 2002). Metabolite profiling requires precise and high dynamic ranges for metabolite identification. LC, GC, and mass spectrometry (MS) have been developed in advance for improved compound identification and classification, whose analytical techniques and equipment are currently underway of more rapid development with automation for more reliable quantification. There are many platforms in metabolic profiling, for example, gas chromatography-mass spectrometry (GC-MS) (Horning and Horning, 1971), liquid chromatography-mass spectrometry (LC-MS) (Lu et al., 2008), and nuclear magnetic resonance spectroscopy (NMR) (Ratcliffe and Shachar-Hill, 2001). Each platform has strengths and weaknesses. For examples, NMR has the advantage of identifying metabolite structures; however, it shows relatively low sensitivity, and thus it can be used for highly abundant metabolites when profiling complex mixtures (Lisec et al., 2006). LC-MS platform can analyze giant metabolites (high molecular weight), but not commonly use specific analyze column condition between LC for interesting molecules. Target molecules must have a suitable form for movement through GC column with gas because GC-MS is a platform for analyzing volatiles. Some of the derivatization methods are developed and applied to metabolomics studies. Silylation is the most suitable derivatization method for non-volatile metabolites such as

hydroxyl and amino compounds (Pierce, 1968). Some silylation agents were tested using the GC-MS platform for plants, which has high reliability and reproducibility. One silylation agent, N-methyl-N-(trimethylsilyl)-trifluoroacetamide (MSTFA) is used to reveal the whole range of metabolites in plants (Fiehn et al., 2000; Lisec et al., 2006). Computer processing of GC-MS data takes advantages of a library search and retention time index for metabolic profiling (Gates and Sweeley, 1978). The advantage of GC-MS system is that it is capable of precise searching of the electron ionizations libraries (Warren, 2011). As mentioned, GC-MS has historically been the most widely applied platform for metabolite profiling.

Metabolomics studies make a significance value from the massive data with non-targeting metabolite analysis, which requires a multivariate statistical analysis. Principal component analysis (PCA) uses an unsupervised method which can provide an overview of the whole metabolite profile and find the differential metabolite profiling within the group using a qualitative analysis (Jackson, 2003; Pearson, 1901). Projections of latent structures (PLS) analysis is a supervised analytical method that enhances the separation between groups, combining variable importance for projection (VIP) scores to obtain a proper cutoff value and increase its performance (Chong and Jun, 2005; Wold et al., 2001). Orthogonal projections of latent structures (OPLS) analysis add a single component to the PLS analysis as a predictor of the model, and the other components describe the variation orthogonal to the first predictive component (Trygg and Wold, 2002; Westerhuis et al., 2009). OPLS-discriminant analysis (DA) provides useful information about putative biomarkers using an S-plot that combines the

covariation and correlation from the model in a scatter plot (Eriksson, 2006; Wiklund et al., 2008). The VIP score in PLS-DA and correlation value in OPLS-DA provide cutoff values for finding significant metabolites(Chong and Jun, 2005). Multivariate data analysis is critical in metabolomics studies for providing a significant clue to the important findings in the numerous experiments.

In this study, profilings of disease-related metabolites are to be examined for characterizing two different pathosystems in the grapevine; the brown leaf spot caused by a necrotrophic fungal pathogen *Pseudocercospora vitis* inducing necrotic symptoms and the crown gall caused by non-necrotrophic (biotrophic) bacterial pathogen *Agrobacterium vitis* inducing hyperplastic symptoms. For the fungal disease, metabolite profiling in four different regions of the grapevine infected with *P. vitis* was analyzed using grapevine cultivar 'Campbell Early', and for the bacterial disease, profiling of disease-related metabolites in stem tissues of 10 grapevine species (cultivars) with differential disease response types were assessed, for both of which GC-MS and multivariate analysis were applied as the analytical instrumentation and statistical validation, respectively. These disease characteristics revealed by metabolite profiling were compared, whose differences and similarities would provide valuable information and new insights on the understandings of the diseases so as to be used for the development of grapevine disease management strategies.

LITERATURE CITED

Aradhya, M.K., Dangl, G.S., Prins, B.H., Boursiquot, J.-M., Walker, M.A., Meredith, C.P. and Simon, C.J. 2003. Genetic structure and differentiation in cultivated grape, *Vitis vinifera* L. Genet. Res. 81: 179–192.

Batovska, D.I., Todorova, I.T., Parushev, S.P., Nedelcheva, D.V., Bankova, V.S., Popov, S.S., Ivanova, I.I. and Batovski, S.A. 2009. Biomarkers for the prediction of the resistance and susceptibility of grapevine leaves to downy mildew. J. Plant Physiol. 166: 781–785.

Burr, T.J. and Otten, L. 1999. CROWN GALL OF GRAPE: Biology and disease management. Annu. Rev. Phytopathol. 37: 53–80.

Burr, T.J., Reid, C.L., Tagliati, E., Bazzi, C. and Süle, S. 1997. Biological control of grape crown gall by strain F2/5 is not associated with agrocin production or competition for attachment sites on grape cells. Phytopathol. 87: 706–711.

Choi, Y.J. and Yun, H.K. 2016. Transcriptional profiles of *Rhizobium vitis*-inoculated and salicylic acid-treated “Tamnara” grapevines based on microarray analysis. J. Plant Biotechnol. 43: 37–48.

Chong, I.G. and Jun, C.H. 2005. Performance of some variable selection methods when multicollinearity is present. Chemom. Intell. Lab. Syst. 78: 103–112.

Creasy, G.L. and Creasy, L.L. 2009. Grapes, 1st edition. ed. CABI, Wallingford, UK; Cambridge, MA.

Dang, J.K. and Daulta, B.S. 1982. Varietal behaviour of grapes to different fungal foliar diseases. Haryana J. Hortic. Sci. 11: 47–52.

Eriksson, L. 2006. Multi- and Megavariate Data Analysis. MKS Umetrics AB.

Ferreira, J.H. and van Zyl, F.G. 1986. Susceptibility of grape-vine rootstocks to strains of *Agrobacterium tumefaciens* biovar 3. South Afr. J. Enol. Vitic. 7: 101–104.

Fiehn, O. 2002. Metabolomics – the link between genotypes and phenotypes. Plant Mol. Biol. 48: 155–171.

Fiehn, O., Kopka, J., Dörmann, P., Altmann, T., Trethewey, R.N. and Willmitzer, L. 2000. Metabolite profiling for plant functional genomics. Nat. Biotechnol. 18, 1157–1161.

Gates, S.C. and Sweeley, C.C. 1978. Quantitative metabolic profiling based on gas chromatography. Clin. Chem. 24: 1663–1673.

Gohlke, J. and Deeken, R. 2014. Plant responses to *Agrobacterium tumefaciens* and crown gall development. Front. Plant Sci. 5

Goodacre, R. 2005. Metabolomics – the way forward. Metabolomics 1, 1–2.

Horning, E.C. and Horning, M.G. 1971. Human metabolic profiles obtained by GC and GC/MS. J. Chromatogr. Sci. 9: 129–140.

Jackson, J.E. 2003. A user's guide to principal components. Wiley-Interscience, Hoboken, N.J.

Jung, S.M., Park, J.H., Park, S.J., Lee, H.C., Lee, J.W. and Ryu, M.S. 2009. Regional differences of leaf spot disease on grapevine cv. "Campbell Early" caused by *Pseudocercospora vitis* in plastic green house. Res. Plant Dis. 15: 193–197.

Kelloniemi, J., Trouvelot, S., Héloir, M.-C., Simon, A., Dalmais, B., Frettinger, P., Cimerman, A., Fermaud, M., Roudet, J., Baulande, S., Bruel, C., Choquer, M., Couvelard, L., Duthieuw, M., Ferrarini, A., Flors, V., Le Pêcheur, P., Loisel, E., Morgant, G., Poussereau, N., Pradier, J.-M., Rascle, C., Trdá, L., Poinssot, B. and Viaud, M. 2015. Analysis of the molecular dialogue between gray mold (*Botrytis cinerea*) and grapevine (*Vitis vinifera*) reveals a clear shift in defense mechanisms during berry ripening. Mol. Plant. Microbe Interact. 28: 1167–1180.

Kim, J.D. and Shin, H.D. 1998. Taxonomic studies on cercospora and allied genera in Korea (I). Kor. J. Mycol. 26: 327–341.

Knapp, D.R. 1979. Handbook of analytical derivatization reactions. John Wiley & Sons.

Kopka, J., Fernie, A., Weckwerth, W., Gibon, Y. and Stitt, M. 2004. Metabolite profiling in plant biology: platforms and destinations. Genome Biol. 5: 109.

Liang, C., Jayawardena, R.S., Zhang, W., Wang, X., Liu, M., Liu, L., Zang, C., Xu, X., Hyde, K.D., Yan, J., Li, X. and Zhao, K. 2016. Identification and characterization of *Pseudocercospora* species causing grapevine leaf spot in China. J. Phytopathol. 164: 75–85.

Lisec, J., Schauer, N., Kopka, J., Willmitzer, L. and Fernie, A.R. 2006. Gas chromatography mass spectrometry–based metabolite profiling in plants. Nat. Protoc. 1: 387–396.

Low, H.H., Gubellini, F., Rivera-Calzada, A., Braun, N., Connery, S., Dujeancourt, A., Lu, F., Redzej, A., Fronzes, R., Orlova, E.V. and Waksman, G. 2014. Structure of a type IV

secretion system. Nature 508: 550–553.

Maia, A.J., Schwan-Estrada, K.R.F., Faria, C.M.D.R., Santos, L.A., Oliveira, J.B.S. and Santos, R.C. 2015. Produção de esporos e efeito da temperatura e luminosidade sobre germinação e infecção de *Pseudocercospora vitis* em videira. Summa Phytopathol. 41: 287–291.

Mullins, M.G., Bouquet, A. and Williams, L.E. 1992. Biology of the Grapevine. Cambridge University Press.

Ophel, K. and Kerr, A. 1990. *Agrobacterium vitis* sp. new species for strains of *Agrobacterium* biovar 3 from grapevines. Int. J. Syst. Bacteriol. 40: 236–241.

Panagopoulos, C.G. and Psallidas, P.G. 1973. Characteristics of Greek isolates of *Agrobacterium tumefaciens* (E. F. Smith & Townsend) Conn. J. Appl. Bacteriol. 36, 233–240.

Park, J.H., Han, K.S., Lee, J.S., Seo, S.T., Jang, H.I. and Kim, H.T. 2006. Effect of temperature on pathogen growth and damage analysis of leaf spot disease on grapevine caused by *Pseudocercospora vitis* in Korea. Res. Plant Dis. 12: 10–14.

Park, J.H., Han, K.S., Lee, J.S., Seo, S.T., Jang, H.I. and Kim, H.T. 2004. Occurrence tendency and decrease of fruits brix according to increasing grapevine leaf spot disease caused by *Pseudocercospora vitis*. Res. Plant Dis. 10: 341–344.

Pearson, K.P. 1901. On lines and planes of closest fit to systems of points in space. Philos. Mag. Ser. 6: 559–572.

Pierce, A.E. 1968. Silylation of organic compounds: a technique for gasphase analysis. Pierce Chemical Company.

Salomone, J.Y., Crouzet, P., De Ruffray, P. and Otten, L. 1996. Characterization and distribution of tartrate utilization genes in the grapevine pathogen *Agrobacterium vitis*. Mol. Plant-Microbe Interact. Mol. Plant. Microbe Interact. 9: 401–408.

Schroth, M.N. 1988. Reduction in yield and vigor of grapevine caused by crown gall disease. Plant Dis. 72: 241.

Sisterna, M. and Ronco, L. 2005. Occurrence of grapevine leaf spot caused by *Pseudocercospora vitis* in Argentina. Plant Pathol. 54: 247–247.

Süle, S. and Burr, T.J. 1998. The effect of resistance of rootstocks to crown gall (*Agrobacterium spp*.) on the susceptibility of scions in grape vine cultivars. Plant Pathol. 47: 84–88.

Sumner, L.W., Mendes, P. and Dixon, R.A. 2003. Plant metabolomics: large-scale phytochemistry in the functional genomics era. Phytochem. 62: 817–836.

Thomma, B.P., Eggermont, K., Penninckx, I.A., Mauch-Mani, B., Vogelsang, R., Cammue, B.P. and Broekaert, W.F. 1998. Separate jasmonate-dependent and salicylate-dependent defense-response pathways in *Arabidopsis* are essential for resistance to distinct microbial pathogens. Proc. Natl. Acad. Sci. 95: 15107–15111.

Trygg, J. and Wold, S. 2002. Orthogonal projections to latent structures (O-PLS). J. Chemom. 16: 119–128.

Warren, C.R. 2011. Use of chemical ionization for GC–MS metabolite profiling. Metabolomics

9: 110–120.

Westerhuis, J.A., Velzen, E.J.J. van, Hoefsloot, H.C.J. and Smilde, A.K. 2009. Multivariate paired data analysis: multilevel PLSDA versus OPLSDA. Metabolomics 6: 119–128.

Wiklund, S., Johansson, E., Sjöström, L., Mellerowicz, E.J., Edlund, U., Shockcor, J.P., Gottfries, J., Moritz, T. and Trygg, J. 2008. Visualization of GC/TOF-MS-based metabolomics data for identification of biochemically interesting compounds using OPLS class models. Anal. Chem. 80: 115–122.

Wilcox, W.F., Gubler, W.D. and Uyemoto, J.K. 2015. Compendium of grape diseases, disorders, and pests, second edition, Amer Phytopathological Society.

Wold, S., Sjöström, M. and Eriksson, L. 2001. PLS-regression: a basic tool of chemometrics. Chemom. Intell. Lab. Syst. 58: 109–130.

Yamada, M. and Sato, A. 2016. Advances in table grape breeding in Japan. Breed. Sci. 66: 34–45.

CHAPTER 1

Metabolic profiles of four different tissues located in grape leaf spot disease caused by *Pseudocercospora vitis*

ABSTRACT

Infected ‘Campbell Early’ grape leaf tissues were collected according to four different tissue locations of brown spot disease: center of leaf spot (A), periphery of leaf spot (C), the uninfected leaf tissue (D) and tissue from A and C as well as the halo (B). Total 118 of metabolites were identified using polar phase GC-MS analysis with sample derivatization and annotated four different sampling tissues. Metabolites were clustered into three groups according to tissues (tissue A, tissue B, and tissues C and D) in the PCA score plot. Tissues C and D were separated to others in the PCA plot; therefore, they had similar metabolite contents variations. Twenty of the metabolites were significantly related to tissues A and C in the S-plot of OPLS-DA. Most of the metabolites, including caffeic acid, succinic acid, and citric acid, were increased in related contents in uninfected tissues (C and D) compared with lesions (A and B). In contrast, D-mannitol, xylitol, and raffinose were increased in the lesion tissues (A and B). Neohesperidin, lactulose, and dehydroascorbic acid were found in the tissue B. As a result; those three metabolites can be expected to be related to the defense mechanism of the grapevine against brown leaf spot disease.

INTRODUCTION

The grape is an important fruit used to make wine and raisins. The grape 'Campbell Early' is a most important table grape cultivar of Korean vineyards, but is susceptible to brown leaf spot disease caused by *Pseudocercospora vitis* (Kim and Shin, 1998). Brown leaf spot disease often causes defoliation of the vine that can be lead to severely decreased grape quality and vine vigor before death (Jung et al., 2009; Park et al., 2004). The disease resistance metabolites in plants are not easily recognized because a lot of primary and secondary metabolites are related to disease resistance, and the metabolic pathways are complicated and linked to each other through various outside stresses.

Many previous studies have searched pathogen-specific chemicals that are known secondary metabolites. Although those secondary metabolites are important in resistance to the pathogen locally, they cannot completely explain metabolite variations on the other side of the plant. Metabolic profiling is a new, useful technique to provide clues within the whole metabolite scale (Sumner et al., 2003). One technique for studying metabolomics is GC-MS. High-resolution separations from the GC column are analyzed, and the precise electron ionizations are searched in libraries (Warren, 2011). Although the GC-MS technique is not sufficient for analysis of high molecular weight compounds, derivatization techniques could help to analysis for some part of metabolites (Knapp, 1979). Some advantages of GC-MS analysis in metabolomics are the well-organized stable protocol from sampling to data analysis and relatively broad coverage of compound classes (Lisec et al., 2006). Silylation is the most

suitable derivatization method for non-volatile metabolites such as hydroxyl and amino compounds (Pierce, 1968). Some silylation agents were tested using the GC-MS platform for plants, which has high reliability and reproducibility. One silylation agent, N-methyl-N-(trimethylsilyl)-trifluoroacetamide (MSTFA) was used to reveal the whole range of metabolites in plants (Fiehn et al., 2000; Roessner et al., 2000; Lisec et al., 2006).

Recently, some metabolomic studies used GC-MS to evaluate disease related metabolites as biomarkers of a particular pathogen, such as downy mildew on grapes (Batovska et al., 2009), Fusarium head blight on wheat (Warth et al., 2014), blast on rice (Johns et al., 2011), bacterial blight on rice (Sana et al., 2010), and *Alternaria brassicicola* on *Arabidopsis* (Botanga et al., 2012). These previous experiments used GC-MS and multivariate data analysis to identify a new aspect for pathogen related metabolites and well-known secondary metabolites. One multivariate data analysis is principal component analysis (PCA), which is an unsupervised method that reduces the dimensionality of the variances (Ericksson et al., 2006). Plots in the multidimensional space are used to determine the similarities and differences between treatment data. Another supervised analysis, orthogonal projections to latent structures discriminant analysis (OPLS-DA), is a recent modification of the Partial Least Squares (PLS) method. This method concentrates its predictive power into the first component to provide an improved model for transparency and interpretability (Ericksson et al., 2006). Multivariate data analysis is critical in metabolomic studies for providing a significant clue to the important findings in the numerous experiments. In this study, we aimed to find the all the pathogen-specific metabolites

against *Pseudocercospora vitis* in the grape cv. ‘Campbell Early’ using GC-MS and multivariate data analysis. Moreover, we also attempted to identify the correlation between the variability of metabolites and disease development using two different multivariate analyses, PCA, and OPLS-DA.

MATERIALS AND METHODS

I. Plant materials

Grape 'Campbell Early' leaves which were clearly developed lesion was collected in the experimental vineyard Suwon Korea at harvest season in 2014. Cleaning and removing contamination of leaf surface with an alcohol soaked paper towel. Leaf tissues were separated to four different tissues on the leaf disease lesion: center of the lesion (A), lesion border (C) the uninfected leaf tissue (D) and tissue from A and C as well as the lesion halo (B) (Figure 1-1). Each leaf tissue sample was made 5 mm leaf disk with a punch immediately put on the liquid nitrogen. Each 20 part of leaf disk tissue was ground in a mortar with LN_2. Each tissue sample was prepared five replicate, and each 50 mg of powder was transferred into a 1.5 ml tube. Ground samples were kept at -80℃ deep freezer and analyzed within one week

II. Sample extraction

Sample preparation method was use modified to Weckwerth (2004). Metabolite extraction was obtained from sampling tube in 1 ml of extraction buffer degassed methanol, chloroform,

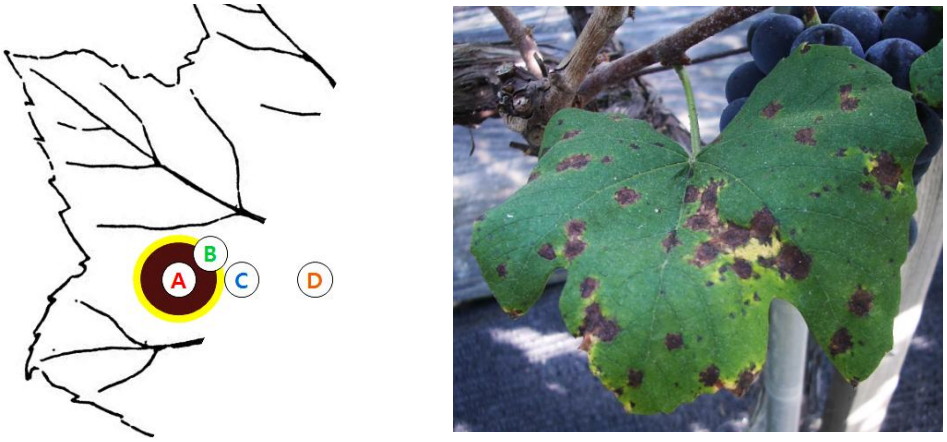

A : Symptom lesion

B : Symptom and symptom lesion border

C : Symptom lesion border

D : Uninfected tissue

Figure 1-1. Brown leaf spot disease caused by *Pseudocercospora vitis* and sampling scheme of the leaf tissues in grape ‘Campbell Early’.

water, (5:2:2, v/v/v) and shaking 5 minutes at 4℃. Extracts centrifuged at 20,000 rpm, the supernatant was transferred new tube, and dried in speed vacuum dryer for 5 hours (Bioneer, Korea). For derivatization, added 20 µl of methoxyamine solution, methoxyamine (Sigma 226904, USA) 20 mg^{-1}·ml pyridine (Sigma 270407, USA) in dried sample tubes and shaking for 90 minutes at 28℃. 180 µl MSTFA (Fluka 68768, Swiss) and 10 µl FAME marker (Supelco C8-C24, USA), use standard retention time marker, were added to each tube and then shaking for 30 minutes at 37℃. Each prepared sample was transferred auto-sampler vial with insert (Supelco #24722, USA).

III. GC-MS analysis

GC-MS system consisted of a gas chromatograph (Agilent 6890, USA) and mass spectrometer (Agilent 5985, USA). 1 µl of sample was injected into a splitless mode, and operating at a temperature of 230 °C at a helium carrier gas flow rate of 1 ml min^{-1}. The column used an HP-5MS, 5% phenyl methyl siloxane. The temperature was 3 min heating at 80°C followed by a 5°C min^{-1} and final 8 min heating at 280°C. Separated ion was detected MS detector at 250°C and recorded at two scans per sec with an m/z 50-600 scan range. One blank sample and One QC samples were injected at the start of an analytical sequence. The analysis order was randomly composed of samples. Data files after GC-MS analysis were treated with deconvolution process by AMDIS (Agilent, USA) with standard parameter (component width = 12; model Ion 0, 73, 207, 281; resolution, sensitivity and shape requirements = medium).

Retention time variation adjusted compare to FAME marker as a retention time standard in a process inside AMDIS program. Peak annotation results were exported text files matched metabolite in the DB. Peak annotation results were matched metabolite in the metabolomics Fiehn DB (Agilent G1676AA, USA) and exported to text files (Kind et al., 2009)

IV. Multivariate analysis

For statistical analysis, each data was treated rescaling which divided by the square root of standard deviation (Pareto scaling; Van den Berg et al., 2006) of each sample variance. Statistical analysis of metabolic profiling with principal component analysis (PCA) and orthogonal projections to latent structures (OPLS) were analyzed by the SIMCA-P+ software (Ver. 12.0, Umetrics, Umea, Sweden; Ericksson et al., 2006).

RESULTS

I. Leaf metabolite differences with unsupervised analysis (PCA)

There were 118 of metabolites on average in each replicated sample when using retention indexing in the metabolic Fiehn library. Metabolites in the different leaf tissues were plotted using PCA (Fig. 1-2). The leaf tissues were plotted in three different groups based on the eigenvector scores, but replicates of tissue C and D samples were plotted together. Two principal components (PC) accounted for 76.4% of total variations, PC1 for 50.7% and PC2 for 25.7%. The PCA model quality was validated based on two variables: R_2X and Q_2X. Our results revealed an R_2X value of 0.764 and a Q_2X value of 0.534. Generally, R_2X values range between 0 and 1, where 1 indicates a model with a perfect fit. Moreover, a Q_2X value > 0.5 indicates a model with good predictability and a value between 0.9-1.0 indicates a model with excellent predictability (Eriksson, 2006). In this PCA, results were used to find metabolite differences between the tissues collected. The PCA is an unsupervised method that attempts to create a model of the data without a priori information; therefore, it can provide an overview of the whole metabolite profile and find the suspected related metabolite among the samples using a qualitative analysis. Thus, PCA does not provide statistically significant evidence for finding a biomarker. In our PCA result, tissues A, B and C separated, but tissues C and D were not separated from each other (Fig. 1-2 A). Tissue C, from the border region of the disease symptom, was expected to contain more highly activated metabolite contents than the other tissues. Tissue

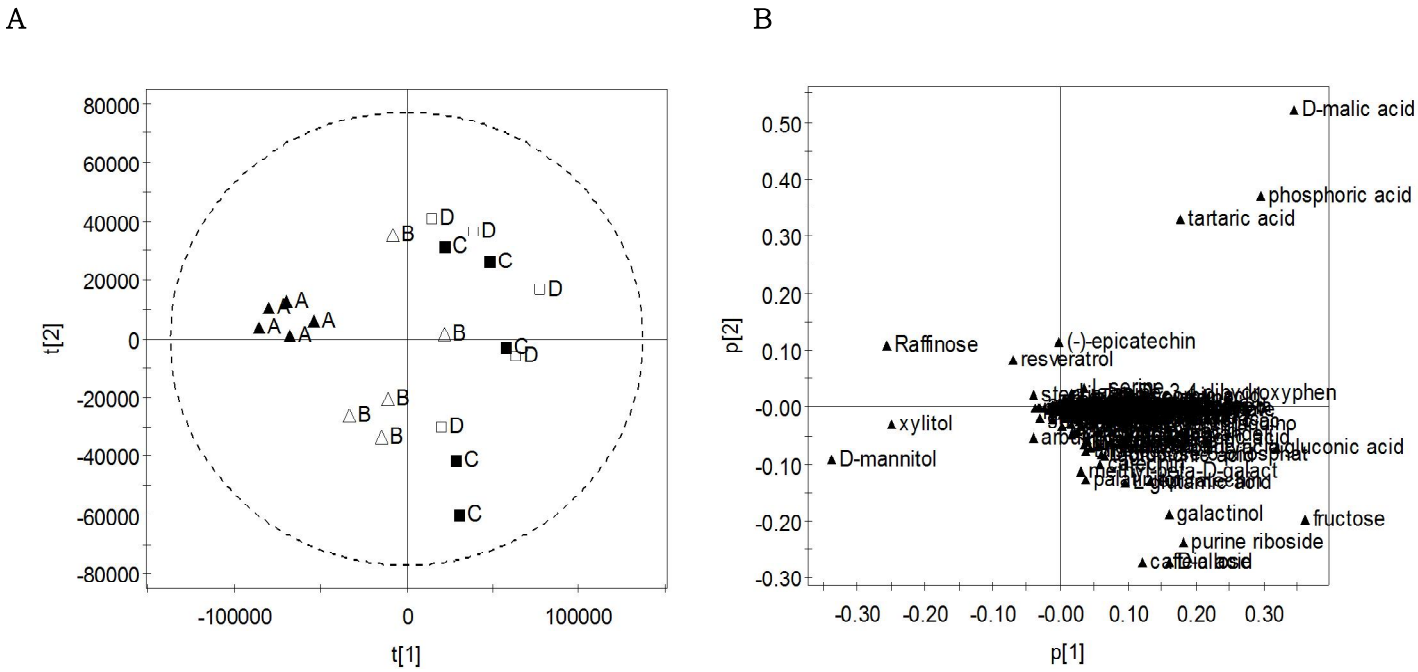

Figure 1-2. Principal component analysis (PCA) plots of four different locations of the leaf tissue of 'Campbell Early' grape infected by *Pseudocecospora vitis*. A. Score plot PC1 (50.7%), PC2 (25.7%), B. loading plot showed just three metabolites weighted to tissue A, but lots of chemicals weighted tissue C and D.

C was not different from tissue D, which looked like normal tissue but was located on the same diseased leaf. Therefore, tissue D already fully produced the defense metabolite against outside invaders like tissue C. Tissue C and D samples were located in the same direction on the PCA score plot (Fig. 1 A) and most of the metabolites related to tissue C and D were weighted on the right side of the PCA loading plot (Fig. 1 B). This result indicated that most of the metabolites of tissues C and D were the same, but the contents of each tissue were different. The PCA loading plot showed that some of the metabolites related to tissue A were raffinose, xylitol, and D-mannitol (Fig. 1 B).

II. Leaf metabolite differences with supervised analysis (OPLS-DA)

The supervised analysis method, OPLS-DA, is similar to PLS-DA, but a single component is used as a predictor for the model and the other components describe the variation orthogonal to the first predictive component (Westerhuis et al., 2010). In this experiment, we collected different tissues from the leaf and tried to find a significant metabolite using OPLS-DA. The S-plot is used to identify the factors that interact with each other in the OPLS-DA model, and the results are useful for identifying a metabolite marker with statistical significance in the different conditions (Wiklund et al., 2008). Before S-plot plotting, data are cut down based on variable importance for projection (VIP) values > 1 and $p < 0.05$ to select for potentially related metabolites. The selected metabolites with VIP values > 1 were associated significantly with the separation shown in both S-plot models, as the functions calculated from the weighted sum of

squares of the PLS weight indicate the importance of the selected variable to the whole model (Azizan et al., 2012).

In this study, a total six different OPLS-DA models were combined for four different leaf tissue samples. Among the six different OPLS-DA models, only three were significantly different from each other based on the metabolite contents (Table 1). The first model (A vs. B) resulted in one predictive and one orthogonal (1 + 2) component with a cross-validated predictive ability Q_2(cum) of 87%, a total explained variance R_2X of 63%, and a variance related to class separation R_2 p(X) of 18%. The second model (A vs. C) resulted in one predictive and three orthogonal components (1 + 2). The predictive ability Q_2(cum) was 95%, the total explained variance R_2X was 69%, and the variance related to the differences between the two classes R_2 p(X) was 14%. The third model (A vs. D) resulted in one predictive and three orthogonal components (1 + 2). The predictive ability Q_2(cum) was 90%, the total explained variance R_2X was 67%, and the variance related to the differences between the two classes R_2 p(X) was 13% (Table 1). Another three models demonstrated the none of the significance into the cross-validated analysis of variance (CV-ANOVA) ($p < 0.05$) and were not clearly separated from each other in the PCA score plot (Fig. 1-1). In general, values of R_2 and $Q_2 > 50\%$ are considered satisfactory for metabolic experiments (Azizan, 2012), but CV-ANOVA uses a statistical diagnosis method in the PLS and OPLS models (Eriksson et al., 2008). Despite that the R_2X and Q_2(cum) were > 50%, models B vs. C and B vs. D showed no significance ($p < 0.05$) in their differences according to CV-ANOVA. We can find a meaningful metabolite to

compare laboriously each metabolite with using an ANOVA test in PCA, but the CV-ANOVA in the OPLS model can help to find a metabolite that is statistically significant between models

Table 1-1. Cross-validation of OPLS-DA models at the tissue compares combination models collected different leaf tissues from grape 'Campbell Early' leaves infected by *Pseudocercospora vitis*.

Model[a]	Fitting values				CV-ANOVA
	Component[b]	R_2X	R_2Y	$Q_{2(cum)}$	*p*
A vs. B	(1+2)	0.630	0.987	0.877	0.048
A vs. C	(1+2)	0.691	0.995	0.949	0.010
A vs. D	(1+2)	0.669	0.990	0.895	0.043
B vs. C	(1+3)	0.548	0.994	0.691	0.296
B vs. D	(1+5)	0.560	0.993	0.524	0.560
C vs. D	(1+3)	0.612	0.992	0.228	0.976

[a] Center of the lesion (A), lesion, a halo of lesion border, and lesion border of the leaf (B), lesion border (C) and not infected leaf tissue (D). Values were calculated with Simca-P.

[b] Component number (predictive + orthogonal).

DISCUSSION

A comparison between tissues A (lesion) and C (border of the lesion) was expected to find a metabolite that was closely linked to brown spot disease in the grape 'Campbell Early'. According to the A vs. C model on the OPLS-DA, a total of 20 metabolites were significantly related to the symptom-lesion and border of the lesion (Fig. 1-3). Of those metabolites, 17 were decreased in the tissue A from the lesion. These metabolites were classified as amino acids, sugars, and organic acids and included D-glucose-6-phosphate, D-allose, fructose, L-glutamic acid, succinic acid, citric acid, D-malic acid, caffeic acid, phosphoric acid, gluconic acid, glyceric acid, catechin, galactinol, epicatechin, and purine-riboside. Most metabolites were included in the basic metabolic pathway as a part of the plant defense system. Both catechin and epicatechin have been reported as part of the grape's disease resistance. D-glucose-6-phosphate is a precursor for hypersensitive reaction and reactive oxygen species (ROS) production against the pathogen (Asai et al., 2011). In addition, D-allose acts a triggering molecule in the pathogen attack (Kano et al., 2013) and gluconic acid has antimicrobial activity and regulates other antimicrobial compound production (Werra et al., 2009).

In contrast, three chemicals, D-mannitol, xylitol, and raffinose, were significantly increased in the center of the lesion. Those chemicals were found similarly to the PCA result (Fig. 1 B). Those chemicals were previously reported to be related to plant and microbe interactions; for example, raffinose is an oligosaccharide that accumulates in plant cells in

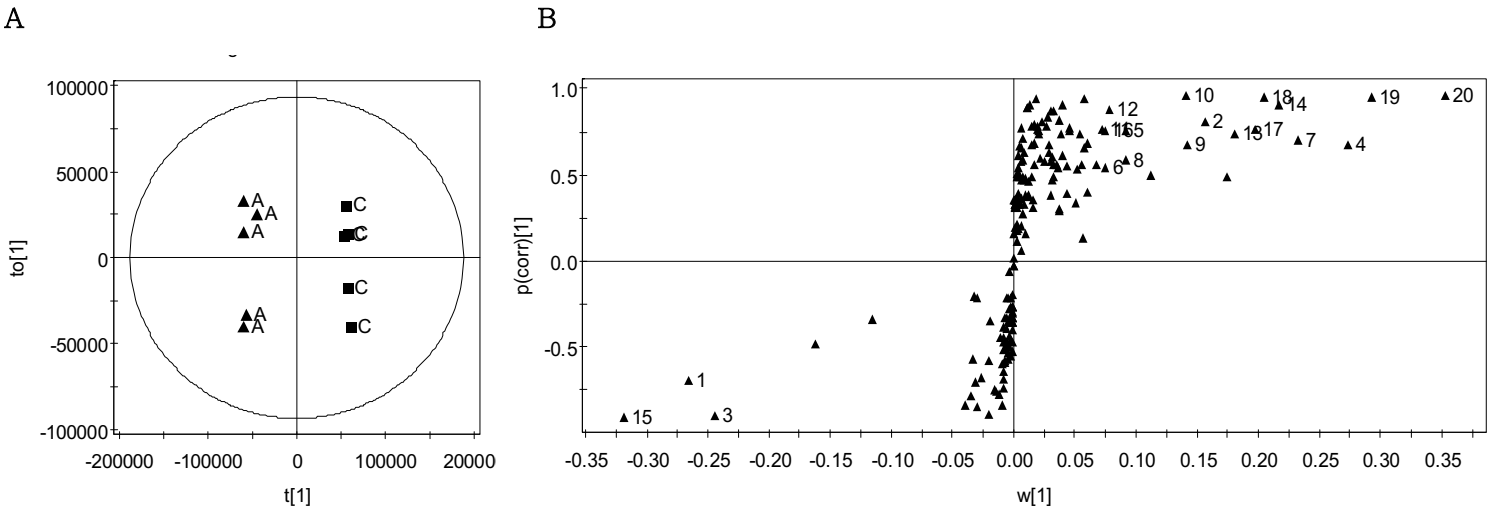

Figure 1-3. Orthogonal projections to latent structures discriminant analysis (OPLS-DA) plots of compare with two of grape 'Campbell Early' leaf tissues infected by *Pseudocecospora vitis*. A. Score plot of OPLS-DA, Variation explained between tissues (69%), within the tissue (14%), B. S-plot of OPLS-DA, The numbered metabolites are a satisfied condition (VIP > 1 and p (corr) $\geq |0.5|$), 1. Raffinose, 2. Galactinol, 3. Xylitol, 4. D-malic acid, 5. L-glutamic acid, 6. Lactose, 7. Phosphoric acid, 8. Palatinitol, 9. Caffeic acid, 10. Glyceric acid, 11. Succinic acid, 12. D-glucose-6-phosphate, 13. Purine riboside, 14. D-allose, 15. D-mannitol, 16. Catechin, 17. Epicatechin, 18. Citric acid, 19. Gluconic acid, 20. Fructose. On the left side numbered chemicals were significantly correlated to tissue A, and numbered chemicals on the right side were correlated to tissue C.

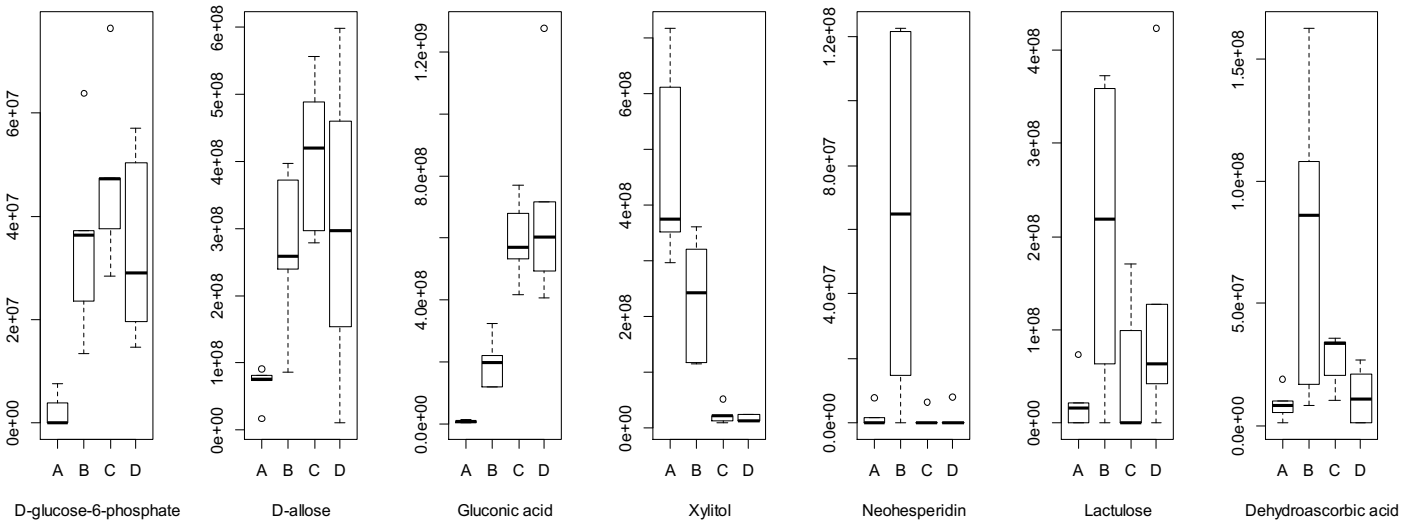

Figure 1-4. Putative metabolites significantly related to the disease were compared with different leaf tissue locations in the grape 'Campbell Early' infected by *Pseudocecospora vitis*. Y axis is a related area in GC-MS peak; X-axis is different infected leaf tissues.

response to environmental stresses (Zhou et al., 2012) and D-mannitol is used to suppress ROS-mediated plant defenses by phytopathogenic fungi (Jennings et al., 1998).The role of xylitol in the plant defense mechanism in grapes is unclear at this time, but it is well-known as an inhibitor of various bacteria.

On the other hand, we used S-plot analysis to find a precise metabolite to tissue B, by comparisons between models (A vs. B and A vs. C). Tissue B contained a yellow halo, which was expected when a specific metabolite had an intense resistance response against the pathogen. We excluded a common metabolite between models A vs. B and models A vs. C and then collected three tissue B-specific metabolites: neohesperidin, lactulose, and dehydroascorbic acid (Fig. 1-3). Those metabolites were highly present in tissue B, including in the halo of the lesion, and are expected to have a strong defense against the pathogen. In the oxidation caused by ultraviolet light in plants, L-ascorbate acts as an anti-oxidant by absorbing active oxygen and turning over dehydroascorbic acid (Parsons and Fry, 2012). In a previous study, the dehydroascorbic acid level was higher in *Arabidopsis* infected with pathogen fungi *Alternaria brassicicola* compared with *Arabidopsis* that was mock inoculated after 24 hours (Botanga et al., 2012). Neohesperidin is an isoflavone, which accumulates to considerable levels in the leaves and fruit of citrus species; although, the biological role of plants is not clear (Frydman et al., 2005). However, lactulose is converted from lactose by beta-galactosidase (Lee et al. 2004), but, unfortunately, there is little known about the role of lactulose in plant disease resistance. These metabolites are expected to be specific for the grape ‘Campbell Early’ and brown spot disease

caused by *Pseudocercospora vitis*. *Cercospora* is closely related to the genus *Pseudocercospora*, and the pathogenicity and disease mechanism in their host have been studied. *Cercospora* spp. produces a photosensitizing fungal toxin cercosporin, which makes singlet oxygen ($^1O_2$) in light (Daub and Hangarter, 1983). As a result, the activated oxygen caused peroxidation of the host plant cell membrane lipids. Finally, nutrients are leaked from the broken host cell membrane (Daub and Ehrenshaft, 2000). In our result showed that both dehydroascorbic acid and neohesperidin had predicted roles in plant disease resistance such as antioxidant process. In conclusion, some metabolites have already been reported to have a part in the defense mechanism in plants, and some have been identified through the statistical analysis. Our results suggested tissue-specific metabolites that may have the potential for use as biomarkers and may provide meaningful information for a different line of research.

LITERATURE CITED

Asai, S., Yoshioka, M., Nomura, H., Tone, C., Nakajima, K., Nakane, E., Doke, N. and Yoshioka, H. 2011. A plastidic glucose-6-phosphate dehydrogenase is responsible for hypersensitive response cell death and reactive oxygen species production. J. Gen. Plant Pathol. 77:152-162.

Azizan, K.A., Baharum, S.N., Ressom, H.W. and Noor, N.M. 2012. GC-MS analysis and PLS-DA validation of the trimethyl silyl derivatization techniques. J. Appl. Sci. 9:1124-1136.

Batovska, D.I., Todorova, I.T., Parushev, S.P., Nedelcheva, D.V., Bankova, V.S., Popov, S.S., Ivanova, II. and Batovski, S.A. 2009 Biomarkers for the prediction of the resistance and susceptibility of grapevine leaves to downy mildew. J. Plant Physiol. 166:781-785.

Botanga, C.J., Bethke, G., Chen, Z., Gallie, D.R., Fiehn, O. and Glazebrook, J. 2012. Metabolite profiling of *Arabidopsis* inoculated with *Alternaria brassicicola* reveals that ascorbate reduces disease severity. Mol. Plant. Microbe Interact. 25:1628-1638.

Daub, M.E. and Ehrenshaft, M. 2000. The photoactivated *Cercospora* toxin cercosporin: contributions to plant disease and fundamental biology. Annu. Rev. Phytopathol. 38:461-490.

Daub, M.E. and Hangarter, R.P. 1983. Light-induced production of singlet oxygen and superoxide by the fungal toxin, cercosporin. Plant physiol. 73: 855-857.

Eriksson, L., Johansson, E., Kettaneh-Wold, N., Trygg, J., Wikstrom, C., Wold, S. 2006. Multi-

and megavariate data analysis. Umetrics AB, Sweden.

Eriksson, L., Trygg, J. and Wold, S. 2008. CV-ANOVA for significance testing of PLS and OPLS models. J. Chemometrics 22:594-600.

Fiehn, O., Kopka, J., Dormann, P., Altmann, T., Trethewey, R. and Willmitzer, L. 2000. Metabolic profiling of plant functional genomics. Nat. Biotechnol. 18:1157-1161.

Frydman, A., Weisshaus, O., Huhman, D.V., Sumner, L.W., Bar-Peled, M., Lewinsohn, E., Fluhr, R., Gressel, J. and Eyal, Y. 2005. Metabolic engineering of plant cells for biotransformation of hesperidin into neohesperidin, a substrate for production of the low-calorie sweetener and flavor enhancer. J. Agric. Food Chem. 53: 9708-9712.

Jennings, D.B., Ehrenshaft, M., Pharr, D.M. and Williamson, J.D. 1998. Roles for mannitol and mannitol dehydrogenase in active oxygen-mediated plant defense. Proc. Natl. Acad. Sci. 95:15129-15133.

Jones, O.A., Maguire, M.L., Griffin, J.L., Jung, Y.H., Shibato, J., Rakwal, R., Agrawal, G.K. and Jwa, N.S. 2011. Using metabolic profiling to assess plant-pathogen interactions an example using rice (*Oryza sativa*) and the blast pathogen Magnaporthe grisea. Eur. J. Plant Pathol. 129:539-554.

Jung, S.M., Park, J.H., Park, S.J., Lee, J.W. and Ryu, M.S. 2009. Regional differences of leaf spot disease on grapevine cv. ‘Campbell Early’ caused by *Pseudocercospora vitis* in plastic green house. Res. Plant Dis. 19:193-197.

Kano, A., Fukumoto, T., Ohtani, K., Yoshihara, A., Ohara, T., Tajima, S., Izumori, K., Tanaka,

K., Ohkouchi, T., Ishida, Y., Nishizawa, Y., Ichimura, K., Tada, Y. and Akimitsu, K. 2013. The rare sugar D-allose acts as a triggering molecule of rice defence via ROS generation. J. Exp. Bot. 64:4939-4951.

Kind, T., Wohlgemuth, G., Lee, D.Y., Lu, Y., Palazoglu, M., Shahbaz, S. and Fiehn, O. 2009. FiehnLib: mass spectral and retention index libraries for metabolomics based on quadrupole and time of flight gas chromatography/mass spectrometry. Anal. Chem. 81:10038-10048.

Kim, J.D. and Shin, H.D. 1998. Taxonomic studies on *Cercospora* and allied genera in Korea (1). Kor. J. Mycol. 26:327-341.

Knapp, D.R. 1979. Handbook of analytical derivatization reaction. Wiley & Sons New York

Lee, Y.J., Kim, C.S. and Oh, D.K. 2004. Lactulose production by beta-galactosidase in permeabilized cells of *Kluyveromyces lactis* – Appl. Microbiol. Biotechnol. 64:787-793.

Lisec, J., Schauer, N., Kopka, J., Willmitzer, L. and Fernie, A.R. 2006. Gas chromatography mass spectrometry-based metabolite profiling in plants. Nat. Protocol. 1:387-396.

Park, J.H., Han, K.S., Lee, J.S., Seo, S.T., Jang, H.I. and Kim, H.T. 2003. Occurrence tendency and decrease of fruits brix according to increasing grapevine leaf spot disease caused by *Pseudocercospora vitis*. Res. Plant Dis. 10:341-344.

Parsons, H. and Fry, S. 2012. Oxidation of dehydroascorbic acid and 2,3-diketogulonate under plant apoplastic condition. Phytochem. 75:41-49.

Pierce, A.E. 1968. Silylation of organic compounds. Pierce chemical company

Roessner, U., Wagner, C., Kopka, J., Trethewey, R.N. and Willmitzer, L. 2000. Simultaneous analysis of metabolites in potato tuber by gas chromatography-mass spectrometry. Plant J. 23:131-142.

Sana, T.R., Fischer, S., Wohlgemuth, G.W., Katrekar, A., Jung, K.H., Ronald, P.C. and Fiehn, O. 2010. Metabolomic and transcriptomic analysis of the rice response to the bacterial blight pathogen *Xanthomonas oryzae pv. Oryzae*. Metabolomics 6:451-465.

Sumner, L., Mendes, P., Dixon, R. 2003. Plant metabolomics: large-scale phytochemistry in the functional genomics era. Phytochem. 62:817-836.

Van den Berg, R., Hoefsloot, H.C.J., Westerhuis, J.A., Smilde, A.K. and Van der Werf, M.J. 2006. Centering, scaling, and transformations: improving the biological information content of metabolomics data. BMC Genomics 7:142-157.

Warren, C.R. 2013. Use of chemical ionization for GC-MS metabolite profiling. Metabolomics 9: 110-120.

Warth, B., Parich, A., Bueschl, C., Schoefbeck, D., Neumann, N.K.N., Kluger, B., Schuster, K., Krska, R., Adam, G., Lemmens, M. and Schuhmacher, R. 2014. GC–MS based targeted metabolic profiling identifies changes in the wheat metabolome following deoxynivalenol treatment. Metabolomics 11:722-738.

Werra, P.D., Pechy-Tarr, M., Keel, C. and Maurhofer, M. 2009. Role of gluconic acid production in the regulation of biocontrol traits of *Pseudomonas fluorescence* CHA0. Appl. Environ. Microbiol. 75: 4162-4174.

Westerhuis, J.A., Van Velzen, E.J.J., Hoefsloot, H.C. and Smilde, A.K. 2010. Multivariate paired data analysis: multilevel PLSDA versus OPLSDA. Metabolomics 6:119-128.

Weckwerth, W., Wenzel, K., Fiehn, O. 2004. Process for the integrated extraction identification and quantification of metabolites proteins and RNA to reveal their co-regulation in biochemical networks. Proteomics 4:78-83.

Wiklund, S., Johansson, E., Sjostrom, L., Mellerowicz, E., Edlund, U., Shockcor, J., Gottfries, J., Moritz, T. and Trygg, J. 2008. Visualization of GC/TOF-MS-based metabolomics data for identification of biochemically interesting compounds using OPLS class models. Anal. Chem. 80:115-122.

Zhou, M.L., Zhang, Q., Zhou, M., Sun, Z.M., Zhu, X.M., Shao, J.R., Tang, Y.X., Wu, Y.M. 2012. Genome-wide identification of genes involved in raffinose metabolism in Maize. Glycobiology 22:1775-1785.

CHAPTER 2

Metabolic profiles of grapevine internode tissues infected with *Agrobacterium vitis*

ABSTRACT

Green shoot cuttings of 10 different grapevine species were inoculated with *Agrobacterium vitis* to find disease-related metabolites in the grapevine. Crown galls formed 60 days after inoculation varied in gall severity (GS) evaluated by gall incidence (GI) and gall diameter (GD), which were classified into three response types as RR (low GI and small GD), SR (high GI and small GD) and SS (high GI and large GD), corresponding to resistant, moderately resistant and susceptible responses, respectively. In this, 4, 4 and 2 *Vitis* species were classified into RR, SR, and SS, respectively. GC-MS analysis of the grapevine stem metabolites with *A. vitis* infection showed 134 metabolites in various compound classes critically occurred, which were differentially clustered with the response types by the principal component analysis (PCA). Multivariate analysis of the metabolite profile revealed that 11 metabolites increased significantly in relation to the response types, mostly at post-inoculation stages, more prevalently (8 metabolites) at two days after inoculation than other stages, and more related to SS (7 metabolites) than RR (3 metabolites) or SR (one metabolite). This suggests most of the disease-related metabolites may be rarely pre-existing but mostly induced by pathogen infection largely for facilitating gall development except stilbene compound resveratrol, a phytoalexin that may be involved in the resistance response. All of these aspects may be used for the selection of resistant grapevine cultivars and their rootstocks for the control of the crown gall disease of the grapevine.

INTRODUCTION

Crown gall of grapevine reduces the grape yield by 20~40% and trunk diameter approximately by 9%, compared to uninfected healthy grapevines (Schroth et al., 1988). The causal agent of the grapevine crown gall, *Agrobacterium vitis*, is a different biovar from other *Agrobacterium spp.* because it can induce a grapevine-specific crown gall (Panagopoulos and Psallidas, 1973). *A. vitis* has host specificity-related genes, such as *pehA,* which encodes polygalacturonase (PG) that is hypothesized to facilitate *A. vitis* attachment and systemic colonization on susceptible grapevine tissues (Burr and Otten, 1999). Another host specificity-related gene function is tartrate utilization, and the host specificity is explained by the use of tartaric acid from specific organic acids in grapevines (Salomone et al., 1996).

Crown gall disease is one of the difficult diseases to eradicate by chemicals in vineyards. As a strategy to prevent crown gall disease without chemical sprays, the use of resistance plant cultivars and antagonistic microbial species have been developed. Some grapevine species, mostly *Vitis vinifera*, are susceptible to crown gall disease, and thus, rootstocks from resistant species or crossed seedlings are used by many vineyards to prevent crown gall disease on the scions of the susceptible grapevine cultivars (Süle and Burr, 1998). Another prevention strategy is the use of a non-tumorigenic *A. vitis* strain as host-specific biological control of grapevine crown gall, in which its pretreatment inhibits transformation by tumorigenic *A. vitis* strains on the grapevine, leading to the inhibition of crown gall induction (Kaewnum et al., 2013; Zauner et al., 2006).

Recently, various platforms have been used to attempt to identify disease resistance-related metabolites in grapevine, including NMR spectroscopy (Browne and Brindle, 2007) and LC-MS (Ehrhardt et al., 2014). However, when using GC-MS, extracted metabolite- profiling data can annotate information from the metabolite libraries (Warren, 2013). Derivatization techniques are required to process GC-MS metabolite profiling (Knapp, 1979). Silylation is the most suitable derivatization method for non-volatile metabolites, such as hydroxyl and amino compounds (Pierce, 1968). One silylation agent, N-methyl-N-(trimethylsilyl)-trifluoro-acetamide (MSTFA), has been used to reveal the whole range of metabolites in plants (Fiehn et al., 2000; Lisec et al., 2006; Roessner et al., 2000). However, the highest advantages of GC-MS analysis in metabolomics are noted as well-organized stable protocols from sampling to data analysis, covering relatively a broad range of compound classes (Lisec et al., 2006).

Principal component analysis (PCA) is an unsupervised method that attempts to create a model of the data without a priori information, which is able to provide an overview of the whole metabolite profile and find the differential metabolite profiling within the group using a qualitative analysis (Pearson, 1901). Projections of latent structures (PLS) analysis is a supervised analytical method that enhances the separation between groups, combining variable importance for projection (VIP) scores to obtain a proper cutoff value and increase its performance (Wold et al., 2001; Chong and Jun, 2005). Orthogonal projections of latent structures (OPLS) analysis add a single component to the PLS analysis as a predictor of the model, and the other components describe the variation orthogonal to the first predictive

component (Westerhuis et al., 2010). OPLS-discriminant analysis (DA) provides useful information about putative biomarkers using an S-plot that combines the covariation and correlation from the model in a scatter plot (Eriksson et al., 2006). The VIP score in PLS-DA and correlation value in OPLS-DA provide cutoff values for finding significant metabolites. This experimental method using GC-MS and multivariate data analysis can identify new aspects of pathogenicity-related metabolites.

Genetic, physiological and morphological changes of the host plant to the infection of *Agrobacterium* species and in the crown gall development have been well documented in relation to plant responses to the tumorigenic bacterium before T-DNA transfer and during gall development (Gohlke and Deeken, 2014). However, relatively little has been studied on those changes occurring in the non-tumorigenic plant tissues that have been influenced by the disease development (gall development), which may broaden the holistic understandings of plant responses to the crown gall pathogen infection and disease development. This may enhance their practical applicability in the disease control; e. g., use of crown gall-resistant rootstocks. Therefore, in the present study, we examined metabolite profiling in the intermodal tissues of grapevine species in relation to plant responses to the crown gall development in grapevines induced by the infection of *A. vitis* using GC-MS and statistical multivariate data analysis.

MATERIALS AND METHODS

I. Grapevines, pathogen, and Pathogen inoculation

Grapevines (10 *Vitis* spp.) used in our study were obtained from the National Clonal Germplasm Repository (NCGR; USDA-ARS, Davis, CA, USA). For *Vitis* spp., 11~22 green shoot cuttings were collected from NCGR fields in June 2015 and placed in a perlite bed for rooting at 25°C with mist for one month. The green shoot cuttings with root systems were transferred to a pot with bed soil for pathogen inoculation test. The pathogen, kindly provided by Dr. Burr, Cornell University, was *Agrobacterium vitis* K306. The bacterium was cultured on potato-dextrose agar (PDA; Difco, USA) at 25°C for three days. The bacterial cultures grown on PDA were collected by the agar surface scratching in sterile distilled water (SDW), and the population density was examined by dilution plate method (Dhingra and Sinclair, 1985), which was diluted with SDW to make a bacterial suspension with a concentration of 10^9 colony-forming units (CFU) ml^{-1}. For inoculation, a wound (about 1.0 mm deep) was made in the internode of the green shoot using a 2-mm-d drill and 10 μl of the bacterial suspension was injected into the wound using a micropipette. After inoculation, the wound site was immediately wrapped with sealing film (Parafilm, WI, USA) and the green shoot cuttings were grown at 25°C in a greenhouse. Symptom development was examined every other day after inoculation throughout the experimental period.

II. Evaluation of responses of *Vitis* species to *A. vitis* K306 infection

Responses of grapevine species (cultivars) to the crown gall pathogen infection were examined at 60 days after inoculation based on the crown gall development, which was estimated by gall severity (GS) index (GSI) that was evaluated by gall incidence (GI) and gall diameter (GD) index (GDI) as GI x GDI that was 0 = 0.0 (no gall), 1 = 0.1-1.5 mm, 3 = 1.5-5.0 mm, and 5 = above 5 mm of GD (Ferreira and vanZyl, 1986), and expressed as averages and standard deviations of 11~22 replications depending on the number of shoot cuttings used for the *Vitis* species tested. The plant responses were classified into different response types based on GI, GD and GSI of *Vitis* species into RR (low GI and small GD), SR (high GI and small GD) and SS (high GI and large GD), respectively, based on significant differences in GSI at $P \leq 0.05$ by Tukey's honest significant difference (HSD) test, corresponding to resistant, moderately resistant and susceptible plant responses to the bacterial infection, respectively.

III. Tissue sampling

Grapevine internodal tissues were sampled at four different stages: pre-inoculation stage (pre); two days before inoculation, postinoculation stage 1 (post 1); two days after inoculation, post 2; seven days after inoculation, and post 3; 30 days after inoculation. For all grapevine species, fresh stem tissues of about 100 mg around the inoculation sites were cut off each from three stem tissues and placed in a 0.5-ml microtube followed by the addition of liquid nitrogen and kept at -80°C in a deep freezer until use.

IV. Extraction of total metabolites from the sampled tissues

Total metabolites were extracted from the frozen tissue samples using a modified extraction method developed by Fiehn et al. (2008). Briefly, about 20 mg of each sample was placed in a 1.5-ml Eppendorf tube containing 1 ml of pre-cooled extraction buffer [degassed methanol, chloroform, water; 5:2:2, v/v/v)]. Samples were macerated at 1,750 rpm for 1 min at 4°C using a ball mill (Retsch corp, MM301). After tissue maceration, the samples were vortexed for 10 sec and shaken for 6 min at 4°C on an orbital mixing plate (Torrey Pines Scientific Instruments). Plant debris was discarded as of the precipitate after centrifuging for 2 min at 14,000 rcf using a bench-top centrifuge at 4°C (Eppendorf 5415D). The supernatant (500 µl) was transferred into a new 1.5-ml Eppendorf tube and dried using a vacuum concentrator (Centrivap cold trap concentrator, Labconco). For derivatization, 20 µl of methoxyamine solution (Sigma 226904, USA) containing 20 mg ml^{-1} pyridine (Sigma 270407, USA) was added to dried sample tubes and shaken for 90 min at 30°C. To each tube, 91 µl MSTFA (Fluka 68768, Swiss) and 10 µl FAME marker (Supelco C8-C24, USA) were added and then shaken for 30 min at 37°C. Each prepared sample was transferred to an autosampler vial with a micro-insert (Supelco #24722, USA).

V. GC-MS analysis

The GC-MS system consisting of a gas chromatograph and mass detector (Leco Pegasus IV

mass spectrometer, USA) was used for GC-MS analysis of the metabolites extracted from the tissue samples. A 0.5 µl sample was injected into the liner in splitless mode, and the liner was exchanged every ten samples. The injection temperature started at 50°C and ramped to 250°C by 12°C per sec. The GC column was a Rtx-5Sil MS (Restek, 30 m x 0.25 mm) at a constant flow of 1 ml min^{-1} helium gas. The column temperature started at 50°C for 1 min and then ramped to 330°C. Automatic mass spectral deconvolution was performed with peak detection of GC spectrum using The BinBase algorithm (rtx5). After peak peaking, peak data were deposited BinBase DB with BinBase ID. BinBase settings: validity of chromatogram (peaks with intensity > 10^7 counts s^{-1}), unbiased retention index marker detection (MS similarity > 800, validity of intensity range for high m/z marker ions), retention index calculation by 5th order polynomial regression. Spectra are cut to 5% base peak abundance and matched to database entries from most to least abundant spectra using the following matching filters: equivalent to about ± 2 s retention time, unique ion must be included in apexing masses and present at > 3% of base peak abundance, mass spectrum similarity must fit criteria dependent on peak purity and signal/noise ratios (5:1). Failed spectra are automatically entered as new database entries if s/n > 25, purity < 1.0 and presence in the biological study design class was > 80%. Resulting .txt files were exported to a data server with absolute spectral intensities and further processed by a filtering algorithm implemented in the metabolomics BinBase DB (Kind et al., 2009).

VI. Multivariate data analysis

For statistical analysis, the spectrum peak data were divided by the square root of the standard deviation of each sample variance (Pareto scaling; Van den Berg et al., 2006). Statistical analysis of metabolic profiles obtained by PCA and OPLS were analyzed using SIMCA-P+ software (Ver. 12.0, Umetrics, Umea, Sweden; Ericksson et al., 2006). Before obtaining the S-plot, potential metabolites related to response types were selected based on VIP score > 1 and $P \leq 0.05$ (Azizan et al., 2012). For these metabolites that were significantly related to response types, their GC-MS data were grouped in three different response types of *Vitis* species (4 RR, 4 SR and 2 SS), of which GC-MS data were analyzed again statistically for their relationships with response types by employing Fisher's least significant difference (LSD) test based on critical values from the t-distribution table at $P \leq 0.05$ (two-tailed), followed by the analysis of variance (ANOVA) in a completely randomized design.

RESULTS

I. Responses of grapevine species to *A. vitis* K306 infection in the inoculation test.

Responses of grapevine species (cultivars) to the crown gall pathogen infection were examined at 60 days after inoculation, forming well or poorly developed galls in the inoculation sites of the grapevine stem internodes (Table 2-1, Figure 2-1). Cultivars' responses could be classified into three response types by Tukey's HSD as susceptible type (SS) (high GSI; high GI and large GD), resistant type (RR) (low GSI; low GI and small GD) and moderately resistant type (SR) (moderate GSI; high GI and low GD) (Table 2-1). In this, two *Vitis* species (*V. hybrid* and *V. flexuosa*) were classified as SS with the highest GSI of 4.46 and 4.29, respectively, four species including *V. amurensis*, *V. vinifera*, *V. coignetiae*, and *V. hybrid* classified as SR with GSI of 2.57 ~ 2.36, and four (*V. riparia*, *V. rupestris*, *V. acerifolia*, and *V. rotundifolia*) as RR with the lowest GSI of 1.50 ~ 0.69, showing significant ($P \leq 0.05$) differences in GSI between SS and RR with SR that was not significantly differentiated from the other two response types (SS and RR) (Table 2-1).

II. GC-MS analysis.

For metabolic profiling of each sampled tissue (with three replications for each *Vitis* species), the GC peaks of the total metabolites were annotated, identifying 134 metabolites in each replicated sample using the metabolomics Fiehn DB (Table 2-2). Among these detectable

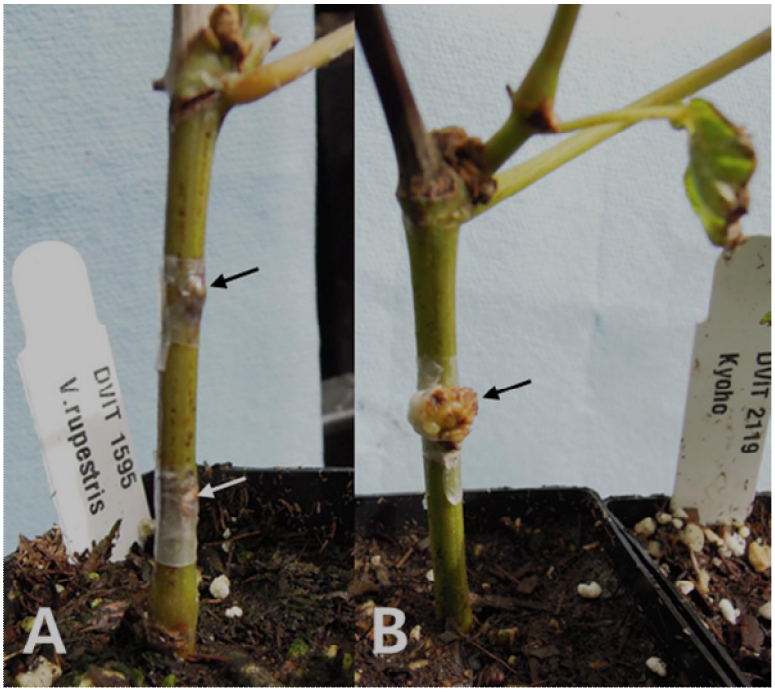

Figure 2-1. Crown gall development on grapevine stem internodes (arrows) with different response types at 30 days after inoculation: A: DVIT 1595 (*Vitis rupestris*) with RR, B: DVIT 2119 (*V. hybrid*) with SS.

Table 2-1. Crown gall formation on grapevines infected with *Agrobacterium vitis* K306 at 30 days after inoculation

ID*	*Vitis* species (cultivar)	Crown gall incidence (GI) (%)	Crown gall diameter (GD) (mm)	Crown gall severity (GS) †	Response type ‡
DVIT 2199	*V.* hybrid (Kyoho)	85.7	13.3 ± 4.9 a	4.46 a	SS
DVIT 1385	*V. flexuosa*	85.7	9.6 ± 3.6 ab	4.29 a	SS
DVIT 1159	*V. coignetiae*	72.7	5.6 ± 1.4 bc	2.57 ab	SR
DVIT 1156	*V. amurensis*	62.5	4.6 ± 1.5 bc	2.55 ab	SR
DVIT 1095	*V. vinifera* (Flame SDS)	57.1	4.4 ± 1.4 bc	2.38 ab	SR
DVIT 2540	*V.* hybrid (Black Rose)	54.5	6.6 ± 2.3 bc	2.36 ab	SR
DVIT 1886	*V. riparia*	37.5	5.3 ± 2.1 bc	1.50 b	RR
DVIT 2191	*V. rotundifolia*	*23.1*	6.2 ± 2.7 bc	1.13 b	RR
DVIT 1399	*V. acerifolia*	18.8	5.0 ± 2.2 bc	0.73 b	RR
DVIT 1595	*V. rupestris*	25.0	4.5 ± 0.5 c	0.69 b	RR

*National Clonal Germplasm Repository ID, USDA-ARS

†GS = Σ(severity index x GI); severity index: 1= GD of 0~1.5 mm, 3 = GD of 1.5~5 mm, 5 = GD above 5 mm (Ferreira and vanZyl, 1986).

‡RR: low GI and small GD; SR: high GI and small GD; SS: high GI and large GD

Means followed by the same letters are not significantly different at $P \leq 0.05$ by Tukey's HSD.

metabolites, the most abundant component class was carboxylic acids that contained 41 metabolites, the least one was alkaloids including only 2 metabolites (nornicotine and xnathosine), and also the other classes identified were 28 amines and amino acids, 37 carbohydrates, 3 flavonoids, 13 lipids and 10 nucleic acids and others such as phenolics, steroids, stilbenes and vitamins (Table 2-2).

III. Multivariate data analysis.

PCA plots revealed clustering patterns of *Vitis* species with three response types at one pre- and three post-inoculation stages, in which each dot represented one tissue sample from one *Vitis* species (Figure 2). This shows the dots of tissue samples from *Vitis* spp. with the same response types distributed in closer distances than those with other response types, indicating the *Vitis* spp. were clustered differentially corresponding to response types depending upon the first and second principal components (metabolites). Significant relations of the spectral peak areas of the detectable metabolites with response types were analyzed by the cross-validation ANOVA (CV-ANOVA) using OPLS-DA, in which 11 metabolites were selected to be significantly related to response types (Supplemantary Table 2-1, Figure 2-1). These metabolites were composed of 5 amino acids, 2 carbohydrates, 2 carboxylic acids, 1 flavonoid, and 1 stilbene, for which the GC-MS data for each of three tissue samples from all 10 *Vitis* species with three response types were analyzed for their significant relationships with response types using LSD (Table 2-3). Based on their significant increases about either or both of the other two

Table 2-2. GC-MS-based metabolite profile in grapevine stem internodes infected with or without *Agrobacterium vitis*

Metabolite classification*	Number	Metabolite names†
Alkaloids	2	Nornicotine, Xanthosine
Amines, Amino acids	28	Ethanolamine, Phenylethylamine, Putrescine, Spermidine, 4-Aminobutyric acid, 5-Hydroxynorvaline, Alanine, Asparagine, Aspartate, beta-Alanine, Citrulline, Glutamine, Glycine, Histidine, Isoleucine, Leucine, Lysine, Methionine, O-Acetylserine, Ornithine, Phenylalanine, Proline, Serine, Threonine, trans-4-Hydroxyproline, Tryptophan, Tyrosine, Valine
Carbohydrates	37	1,2-anhydro-myo-Inositol, Arabitol, beta-Gentiobiose, Cellobiose, Dehydroascorbic acid, Fructose, Fructose-6-phosphate, Galactinol, Galactose-6-phosphate, Galactosylglycerol, Glucoheptulose, Glucose, Glucose-1-phosphate, Glucose-6-phosphate, Hexitol, Hexose-6-phosphate, Inositol-4-phosphate, Levoglucosan, Maltose, Maltotriose, Mannose-6-phosphate, Melezitose, Methyl hexopyranoside, Mucic acid, myo-Inositol, N-acetyl-D-Galactosamine, n-acetyl-d-Hexosamine, N-Acetylmannosamine, Pentitol, Raffinose, Ribonic acid, Ribose, Sucrose, Threonic acid, Trehalose, Xylose
Carboxylic acids	41	2,3-Dihydroxybutanoic acid, 2-Deoxytetronic acid, 2-Hydroxyglutaric acid, 3,4-Dihydroxybenzoic acid, 3,4-Dihydroxycinnamic acid, Aconitic acid, alpha-Ketoglutarate, Arachidic acid, Benzoic acid, cis-Caffeic acid, Citramalic acid, Cyanoalanine, Erythronic acid lactone, Ferulic acid, Fumaric acid, Galactonic acid, Luconic acid, Glutaric acid, Glyceric acid, Glycolic acid, Heptadecanoic acid, Hexaric acid, Isocitric acid, Isohexonic acid, Lactic acid, Malic acid, Mannonic acid, Montanic acid, Nicotianamine, Nicotinic acid, Oxalic acid, Pelargonic acid, Phosphopyruvic acid, Pipecolinic acid, Pyruvic acid, Quinic acid, Salicylic acid, Shikimic acid, Succinic acid, Tartaric acid, Xylonic acid
Flavonoids	3	Catechin, Epicatechin, Gallocatechin
Lipids	13	Capric acid, Cerotinic acid, Dodecanol, Isothreonic acid, Lauric acid, Lignoceric acid, Linoleic acid, Linolenic acid, Octadecanol, Oleic acid, Palmitic acid, Stearic acid, Triacontanol
Nucleic acids, Phenols, Steroids, Stilbenes, Vitamins	10	Adenosine, Uracil, Uridine, Phenol, Pyrogallol, beta-Sitosterol, Stigmasterol, Resveratrol, alpha-Tocopherol, gamma-Tocopherol
Total	134	

*Metabolite classification using PubChem (https://pubchem.ncbi.nlm.nih.gov) and ChEBI metabolite ontology DB (http://www.ebi .ac.uk/ols/index)

†peak detection of GC spectrum used The BinBase algorithm (rtx5) and was deposited BinBase DB with Binbase ID after peak peaking. BinBase settings: validity of chromatogram (peaks with intensity $>10^7$ counts s^{-1}), unbiased retention index marker detection (MS similarity>800, the validity of intensity range for high m/z marker ions), retention index calculation by 5th order polynomial regression. Spectra are cut to 5% base peak abundance and matched to database entries from most to least abundant spectra using the following matching filters: equivalent to about ± 2 s retention time, unique ion must be included in apexing masses and present at >3% of base peak abundance, mass spectrum similarity must fit criteria dependent on peak purity and signal/noise ratios (5:1). Failed spectra are automatically entered as new database entries if s/n >25, purity <1.0 and presence in the biological study design class was >80%.

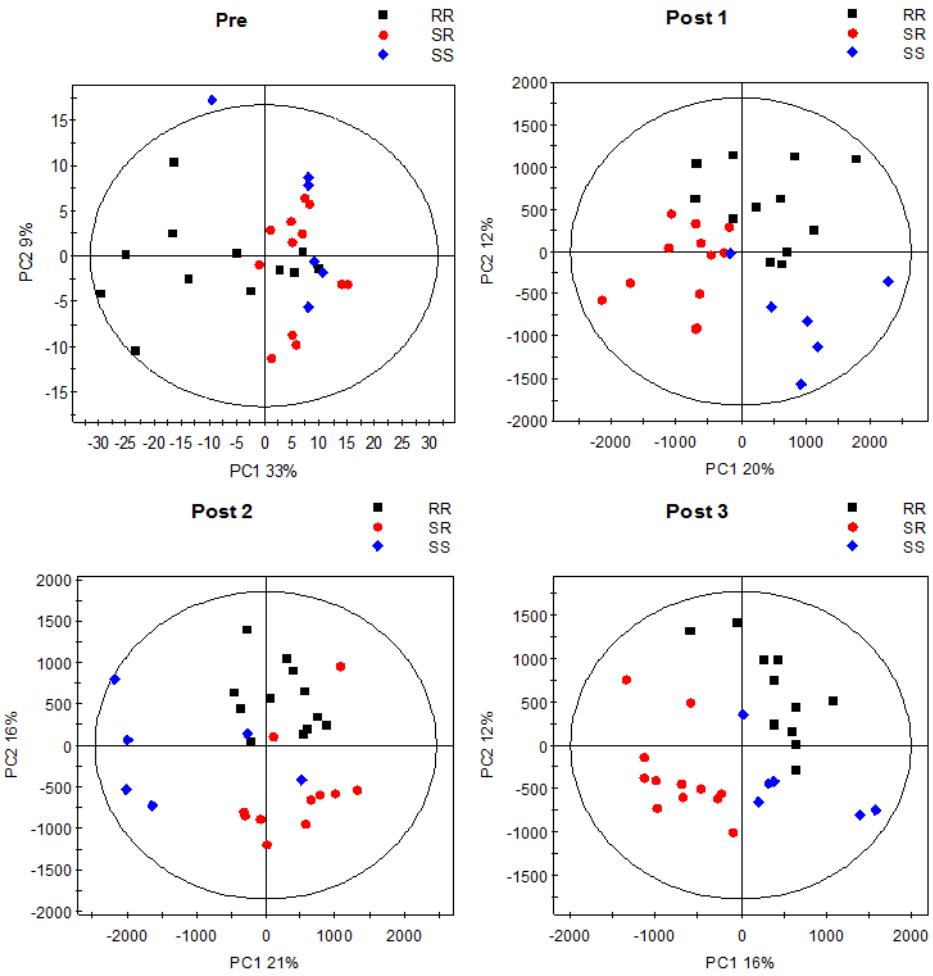

Figure 2-2. PCA plots of three different response groups at pre and post inoculation stages with crown gall disease.

response types, one metabolite (cellobiose) was significantly increased in RR relative to SR at pre-inoculation stage; four (asparagine, gallocatechin, tyrosine, and cellobiose) significantly increased in SS relative to other response types, two (glutamine and histidine) in SS relative to SR, and two (sucrose and resveratrol) in RR or SR relative to SS at post 1; all three metabolites (cellobiose, gallocatechin, and quinic acid) increased in SS relative to SR and/or RR at post 2; and two (valine and xylonic acid) increased in RR relative to SR and other two response types, respectively, and one (sucrose) in SR relative to RR at post 3 (Table 2-3). Totally among the 11 metabolites, seven metabolites increased in SS and 4 in RR at post-inoculation stages, while at pre-inoculation stage (in healthy non-inoculated plants) only one metabolite (cellobiose) was increased in RR, which was also significantly increased in SS at post-inoculation stages (Table 2-3).

Table 2-3. Relative abundance of the GC-MS-based metabolite profiling in grapevine stem internodes in responses to the infection *Agrobacterium vitis* K306 at different infection stages

Stage*	Metabolite†	Component class	Relative abundance (x 10^{-3})‡ Response types		
			RR	SR	SS
Pre	Cellobiose	Carbohydrate	24.12±8.73 a	15.65±6.21 b	24.07±12.28 ab
Post-1	Asparagine	Amino acid	13.57±11.62 b	13.75±13.68 b	36.99±27.64 a
	Gallocatechin	Flavonoid	1.85± 1.47 b	7.28±9.69 b	28.33±28.29 a
	Glutamine	Amino acid	11.09± 6.53 ab	7.75±6.54 b	29.13±19.42 a
	Histidine	Amino acid	20.72±28.01 ab	8.60±8.96 b	45.31±24.35 a
	Tyrosine	Amino acid	3.55 ± 1.60 b	2.85±2.18 b	8.47±5.21 a
	Sucrose	Carbohydrate	400.92±103.56 a	464.78±185.92 a	236.49±220.86 b
	Cellobiose	Carbohydrate	14.32±5.71 b	12.15±7.10 b	27.42±10.66 a
	Resveratol	Stilbenoid	38.49±27.99 a	10.03±10.57 b	17.31±11.72 b
Post-2	Cellobiose	Carbohydrate	12.71±5.27 b	15.19±11.98 b	34.22±14.65 a
	Gallochatechin	Flavonoid	1.85±2.45 b	1.54±1.51 b	74.00±49.95 a
	Quinic acid	Carboxylic acid	9.89±3.92 b	12.83±11.95 ab	20.15±14.62 a
Post-3	Valine	Amino acid	53.79±13.65 a	30.05±9.82 b	48.35±16.77 ab
	Xylonic acid	Carboxylic acid	5.83±3.27 a	2.54±0.99 b	2.61±0.77 b
	Sucrose	Carbohydrate	117.41±104.02 b	323.42±149.42 a	209.32±153.81 ab

*Pre; 2 days before inoculation, Post-1; 2 days after inoculation, Post-2; 7 days after inoculation, Post-3; 30 days after inoculation.

†Metabolites significantly increased or decreased in the response types at a specific stage.

‡Relative abundances are averages and standard deviations of three replications each cultivar. Response groups are containing two or four cultivars; RR (*V.riparia, V. rotundifolia, V. acerifolia, V. rupestris*), SR (*V. coignetiae, V. amurensis, V. vinifera*, Black Rose), SS (Kyoho, *V. flexuosa*).

Means followed by the same letters are not significantly different at $P \leq 0.05$ by Least significant difference (LSD) test.

DISCUSSION

A variety of previous studies on crown gall disease resistance revealed variable experimental results depending on the pathogen biovars and grapevine genotypes (Dercks and Creasy, 1989; Mahmoodzadeh et al., 2004; Roh et al., 2003; Stover et al., 1997; Süle et al., 1994). Previously, the crown gall resistance locus (*Rcg1*) was found in the genome of *V. amurensis* (Kuczmog et al., 2012), but subspecies of *V. amurensis* show variable degrees of resistance against different *A. vitis* isolates (Ferreira and vanZyl, 1986; Stover et al., 1997; Szegedi et al., 1984). *V. flexuosa* is an East-Asian grapevine species with high resistance to crown gall disease (Szegedi et al., 1984); however, it was susceptible to *A. vitis*, forming large galls with high gall incidences in our study. Thus, pathogen biovars and plant genotypes should be determined before the use of resistant plant cultivars as tools for plant protection against the crown gall disease.

Plant resistance, as one of control means, is interference with certain stages in the development of a disease cycle (Agrios, 2005). The crown gall disease cycle is composed of pathogen attachment to the wounded plant cells and tissues, T-DNA transfer, integration into the host genome, the expression of virulence genes (*vir*), and production of phytohormones, which can be differentiated into the initial infection stages up to T-DNA integration for host cell transformation (before T-DNA transfer) and later stages of gall developmental resulting from cellular hyperplasia and hypertrophy (Agrios, 2005; Gohlke and Deeken, 2014; Süle et al., 1994).

At the molecular level for resistance in initial infection stages, a lack of bacterial propagation, induction of *vir*, and incomplete integration of T-DNA result in crown gall resistance in grapevines (Gelvin, 2010). *V. riparia* that showed RR in our study had a broad range of crown gall resistance by particularly inhibiting the integration of *A. vitis* T-DNA into plant chromosome (Süle et al., 1994; Stover et al., 1997). This type of resistance prevents the pathogen from infection, resulting in the reduced GI, leading to no or little gall development to have also lowered GDI, which may be applied as a major resistance mechanism for the four *Vitis* species of RR. For SR, GI was similar to SS, but GDI, to RR, suggesting the pathogen infection in SR occurs as in SS, but gall development is retarded as in RR to have moderate GSI between SS and RR. For SS, both *A. vitis* T-DNA integration into host genome and expression of encoded plant oncogenes and increase in phytohormone levels occur readily, resulting in the formation of tumors and their proliferation (Gohlke and Deeken, 2014).

Out of a total 134 metabolites produced in the grapevine stem internodes infected with *A. vitis* K306, 11 metabolites were significantly related with response types of 10 *Vitis* species examined in our study. At pre-inoculation stage, only one metabolite (cellobiose) was significantly increased in RR relative to SR, while all 11 metabolites were significantly increased in either SS or RR at post-inoculation stages, suggesting metabolic changes may occur preferentially around the infection sites after the pathogen infection, especially at initial stages of the pathogen infection (at 2 days after inoculation in our study) with response type-related 8 metabolites, of which 6 (4 amino acids, 1 flavonoid, and 1 carbohydrate) related to SS but only

2 most significantly related to RR (resveratrol; phenolic) and SR (sucrose; carbohydrate). At post 2 (at 7 days after inoculation), all three metabolites (one for each of carbohydrate, carboxylic acid, and flavonoid) were more related to SS than RR or SR; however, at post 3 (30 days after inoculation inoculation) all three metabolites (amino acid, carboxylic acid, and carbohydrate) were more related to RR or SR than SR and/or SS. These all suggest that the metabolic changes occur actively in relation to susceptible responses at the initial stages of the pathogen infection but in relation to resistant responses at later infection stages with full gall development.

An amine derivative, octopine, produced by the octopine-type *A. vitis* used in our study (Burr et al., 1999) and two plant hormones, auxin and cytokinin, produced in the T-DNA transformed plant cells, drive the uncontrolled gall development, determining gall morphology depending on the ratios of the plant hormones (Gohlke and Deeken, 2014; Morris, 1986; Smits et al., 2008). However, neither octopine and its amino acid component arginine nor the plant hormones were produced in a significant level around the infection sites in our study, suggesting the gall-inducing metabolites may hardly be transported out of the tumorigenic tissues. However, the component class most abundantly produced in relation to response types was amino acid in our study, including four amino acids (asparagine, glutamine, histidine, and tyrosine) produced at post 1 and one (valine) at post 3, which was significantly related to SS and RR, respectively. The functions of these amino acids in crown gall development have not been clearly understood, but amino acids are generally involved in the primary metabolism of all living organisms, and

the developing tumor becomes a metabolic sink accumulating metabolites to be supplied in a priority for its growth by the induction of vascular tissue differentiation around gall surface (Aloni et al., 1995). It was reported previously that three SS-related amino acids except tyrosine increase several folds in tumor tissue at later infection stage (35 days after *Agrobacterium tumefaciens* infection) (Deeken et. al., 2006), suggesting also these SS-related amino acids should be related to the gall development, although the time for the production of the materials may differ depending on *Agrobacterium* species. Other component classes of the metabolites such as carbohydrates and carboxylic acids which were increased in SS at 2 and 7 days after inoculation, respectively, may also serve for the gall growth and differentiation by inducing *vir* genes; gallocatechin, a flavonoid, may be involved in the gall formation as a potential auxin transport regulator as in root nodulation and root-knot gall formation (Wasson et al., 2006, 2009). Quinic acid, catechins, and stilbene are related to Pierce's disease, showing these metabolites occur at great levels in xylem tissues of the grapevine infected with *Xylella fastidiosa* (Wallis and Chen, 2012; Wallis et al., 2013).

In plants, major resistance-related responses (defense responses) to *Agrobacterium* spp. occur at two periods of time, initially at the time of recognizing the tumorigenic pathogens and later during the time of the pathogenesis (gall development) in which auxin and cytokinin cause an increase of ethylene that together with salicylic acid inhibits agrobacterial virulence (Gohlke and Deeken, 2014). In our study, resveratrol at post 1 and valine and xylonic acid at post 3 were definitely differentiated as RR from the other response types (Table 3). Resveratrol is a

stilbenoid, a type of natural phenol, and a phytoalexin (known as a plant defense-related material in resistant plants) produced naturally by several plants in response to injury or pathogen infection (Fremont, 2000; Gatto et al., 2008). In grapevine, resveratrol is primarily found in the grape skin and produced as phytoalexin in grapes infected with the grey mold pathogen, *Botrytis cinerea*, of which the accumulation amounts vary with grapevine genotypes, their geographic origin, and exposure to fungal infection (Favaron et al., 2009; Mattivi et al., 1995). Considering the biological characteristics of this stilbene compound (resveratrol), this metabolite may be produced in *Vitis* species with RR at a significant amount and act as a phytoalexin to inhibit the growth and virulence of the tumorigenic pathogen (*A. vitis*) probably more at initial infection stages. For the other metabolites increased in *Vitis* spp. with RR at the later infection stages (30 days after inoculation), valine (amino acid) and xylonic acid (carboxylic acid), their roles in plant responses are not clearly understood. Alterations in the plant metabolism in response to different pathogen infections may function as either supporting the ongoing defense mechanism to lead an efficient resistance response or being exploited by the pathogen to facilitate infection as can be seen in plant glutamate metabolism (Seifi et al., 2013). Thus, it is not an unusual thing that the metabolites in the same compound classes were differentiated in relation to the opposing response types; xylonic acid significantly related to RR at post 3, while quinic acid to SS at post 2; valine related to RR at post 3, while four amino acids (asparagine, glutamine, histidine, and tyrosine) to SS at post 1 in our study. Considering the same class metabolites concomitantly occurred in relation to different response types at

different infection stages, the same class metabolites may play different roles depending on their requirements for *in situ* metabolism, leading to either compatible or incompatible responses to the pathogen infection

In our study, sucrose contents were highest in grapevine stem internodes with SR at post 1 and post 3, which was significantly differentiated from SS at post 1 and RR at post 3, respectively (Table 3). Considering the increased expression of sucrose degradation enzyme genes in gall tissues of *Arabidopsis* and its induction of *Agrobacterium* virulence genes (Cangelosis et al., 1990; Deeken et al., 2006), the increased sucrose contents may support its intake into the metabolic sink, crown gall tissue, contributing to the gall development in different degrees depending on infection stages (Aloni et al., 1998). Host sucrose, synthesized from photosynthetic products (glucose) in the cytoplasm of aerial plant parts, is transported to tumor cells apoplastically and the sucrose contents in phloem sap differ depending on the crown gall-developmental stages with higher around actively growing young galls than old matured ones (Malsy et. al., 1992; Mistrik et al., 2000). In our study, the sucrose contents fluctuated with time after infection and were higher at post 1 than post 3, regardless of response types, suggesting the uptake of sucrose should be required for the gall development. Another carbohydrate cellobiose was significantly higher in RR relative to SR at preinfectional stages, but higher in SS than RR and SR at post 1, suggesting its roles in healthy plant tissues may alter oppositely in diseased plant tissues with uncontrolled gall development.

In our study, metabolite profile analysis revealed the following aspects: Remarkable

differential increases of metabolites (11 metabolites) occurred in internodes of *Vitis* species after *A. vitis* infection, most prevalently (8 metabolites) at two days after inoculation, and more related to susceptible type of response (SS) for 10 metabolites that are useful for the metabolic processes in gall growth and differentiation as nutritional compounds or plant hormone regulator. Among three metabolites (resveratrol, valine, and xylonic acid) definitely differentiated into the resistant response (RR), resveratrol appeared to be importantly related to resistant responses as it is a well-known phytoalexin compound in several plant pathosystems. All of these aspects will provide important information that can be applied for the selection of grapevine cultivars resistant to the crown gall disease caused by *A. vitis*, and their use as rootstocks for the control of the crown gall disease in the scions of the grapevines susceptible to *A. vitis*.

LITERATURE CITED

Agrios, G. N. 2005. Plant pathology, 5th ed. Academic Press, San Diego, CA. USA. 922pp.

Aloni, R., Pradel, K. S. and Ullrich, C. I. 1995. The three-dimensional structure of vascular tissues in *Agrobacterium tumefaciens*-induced crown galls and in the host stems of *Ricinus communis* L. Planta 196: 597-605.

Aloni, R., Wolf, A., Feigenbaum, P., Avni, A. and Klee, H. J. 1998. The never ripe mutant provides evidence that tumor-induced ethylene controls the morphogenesis of *Agrobacterium tumefaciens*-induced crown galls on tomato stems. Plant Physiol. 117:841-849.

Azizan, K.A., Baharum, S.N., Ressom, H.W. and Noor, N.M. 2012. GC-MS analysis and PLS-DA validation of the trimethylsilyl derivatization techniques. J. Appl. Sci. 9:1124-1136.

Browne, R.A. and Brindle, K.M. 2007. 1H NMR-based metabolite profiling as a potential selection tool for breeding passive resistance against Fusarium head blight (FHB) in wheat. Mol. Plant Pathol. 8:401-410.

Burr, T.J. and Otten, L. 1999. Crown gall of grape: Biology and disease management. Annu. Rev. Phytopathol. 37:53-80.

Burr, T.J., Reid, C.L., Adams, C.E. and Momol, E.A. 1999. Characterization of *Agrobacterium vitis* strains isolated from feral *Vitis riparia*. Plant Dis. 83:102-107.

Cangelosi, G.A., Ankenbauer, R.G. and Nester, E.W. 1990. Sugars induce the *Agrobacterium*

virulence genes a periplasmic binding protein and a transmembrane signal protein. Proc. Natl. Acad. Sci. 87:6708-6712.

Chong, I.G. and Jun, C.H. 2005. Performance of some variable selection methods when multicollinearity is present. Chemometr. Intell. Lab. 78:103-112.

Deeken, R., Engelmann, J. C., Efetova, M., Czirjak, T., Müller, T., Kaiser, W. M., et al. 2006. An integrated view of gene expression and solute profiles of *Arabidopsis* tumors: a genome-wide approach. Plant Cell 18:3617-3634.

Dercks, W. and Creasy, L. 1989. The significance of stilbene phytoalexins in the *Plasmopara viticola*-grapevine interaction. Physiol. Mol. Plant Pathol. 34: 189-202.

Dhingra, O. D. and Sinclair, J. B. 1985. Basic plant pathology methods. CRC Press, Inc., Boca Raton, FL, USA. 355 pp.

Ehrhardt, C., Arapitsas P., Stefanini, M., Flick, G. and Mattivi, F. 2014. Analysis of the phenolic composition of fungus resistant grape varieties cultivated in Italy and Germany using UHPLC-MS/MS. J. Mass Spectrom. 49:860-869.

Eriksson, L., Johansson, E., Kettaneh-Wold, N., Trygg, J., Wikstrom, C. and Wold, S. 2006. Multi- and megavariate data analysis. Umetrics AB, Sweden.

Favaron, F., Lucchetta, M., Odorizzi, S., Pais da Cunha, A.T., Sella, L. 2009. The role of grape polyphenols on *trans*-resveratrol activity against *Botrytis cinerea* and of fungal laccase on the solubility of putative grape PR proteins. J. Plant Pathol. 91: 579–588.

Ferreira, J. H. S. and vanZyl, F. G. H. 1986. Susceptibility of grapevine rootstocks to strains of

Agrobacterium tumefaciens biovar. South Afr. J. Enol. Viticul. 7:101-104.

Fiehn, O., Kopka, J., Dormann, P., Altmann, T., Trethewey, R. and Willmitzer, L. 2000. Metabolic profiling of plant functional genomics. Nat. Biotechnol. 18:1157-1161.

Fiehn, O., Wohlgemuth, G., Scholz, M., Kind, T., Lee, D.Y., Lu, Y., Moon, S. and Nikolau, B. 2008. Quality control for plant metabolomics: reporting MSI-compliant studies. Plant J. 53:691-704.

Fremont, L. 2000. Biological effects of resveratrol. Life Sci. 66: 663–673.

Gatto, P., Vrhovsek, U., Muth, J., Segala, C., Romualdi, C., Fontana, P., Pruefer, D., Stefanini, M., Moser, C., Mattivi, F. and Velasco, R. 2008. Ripening and genotype control stilbene accumulation in healthy grapes. J. Agric. Food Chem. 56: 11773-1185.

Gelvin S. B. 2010. Plant proteins involved in *Agrobacterium*-mediated genetic transformation. Annu. Rev. Phytopathol. 48:45–68.

Gohlke, J. and Deeken, R. 2014. Plant responses to *Agrobacterium tumefaciens* and crown gall development. Plant Sci. 5:1-11.

Kaewnum, S., Zheng, D., Reid, C. L., Johnson, K. L., Gee, J. C. and Burr, T. J. 2013. A host-specific biological control of grape crown gall by *Agrobacterium vitis* strain F2/5: Its regulation and population dynamics. Phytopathology 103: 427-435.

Kind, T., Wohlgemuth, G., Lee, D.Y., Lu, Y., Palazoglu, M., Shahbaz, S. and Fiehn, O. 2009. FiehnLib: mass spectral and retention index libraries for metabolomics based on quadrupole and time of flight gas chromatography/mass spectrometry. Anal. Chem.

81:10038-10048.

Knapp, D.R. 1979. Handbook of analytical derivatization reaction. Wiley & Sons, New York.

Kuczmog, A., Galambos, A., Horváth, S. Mátai, A., Kozma, P., Szegedi, E. and Putnoky, P. 2012. Mapping of crown gall resistance locus *Rcg1* in grapevine. Theor. Appl. Genet. 125:1565-1574.

Lisec, J., Schauer, N., Kopka, J., Willmitzer, L. and Fernie, A.R. 2006. Gas chromatography mass spectrometry-based metabolite profiling in plants. Nat. Protocol. 1:387-396.

Mahmoodzadeh, H., Nazemieh, A., Majidi, I., Paygami, I. and Khalighi, A. 2004. Evaluation of crown gall resistance in *Vitis vinifera* and hybrids of *Vitis spp.* Vitis 43:75-79.

Malsy, S., Van Bel, F., Kluge, M., Hartung, W. and Ullrich, C.I. 1992. Induction of crown galls by *Agrobacterium tumefaciens* (strain C58) reverses assimilate translocation and accumulation in *Kalanchoë daigremontiana.* Plant Cell Environ. 15:519-529.

Mattivi, F., Reniero, F., and Korhammer, S. 1995. Isolation, characterization, and evolution in red wine vinification of resveratrol monomers. J. Agric. Food Chem. 43: 1820–1823.

Mistrik, I., Pavlovkin, J., Wächter, R., Pradel, K.S., Schwalm, K., Hartung, W., Mathesius, U., Stohr, C. and Ullrich, C.I. 2000. Impact of *Agrobacterium tumefaciens*-induced stem tumors on NO_3^- uptake in *Ricinus communis*. Plant Soil 226: 87-98.

Morris, R.O. 1986. Genes specifying auxin and cytokinin biosynthesis in phytopathogens. Annu. Rev. Plant Physiol. 37:509-538.

Panagopoulos, C.G. and Psallidas, P.G. 1973. Characteristics of Greek isolates of

Agrobacterium tumefaciens (E.F. Smith & Townsend) Conn. J. Appl. Microbiol. 36:233-240.

Pearson, K. 1901. On lines and planes of closest fit to systems of points in space. Phil. Mag. 2: 559–572.

Pierce, A.E. 1968. Silylation of organic compounds. Pierce Chemical Company

Roessner, U., Wagner, C., Kopka, J., Trethewey, R.N. and Willmitzer, L. 2000. Simultaneous analysis of metabolites in potato tuber by gas chromatography-mass spectrometry. Plant J. 23:131-142.

Roh, J.H., Yun, H.K., Park, K.S., Lee, C.H. and Jeong, S.B. 2003. In vivo evaluation of resistance of grape varieties to crown gall disease. Plant Pathol. J. 19:235-238.

Salomone, J., Crouzet, P., De Ruffray, P. and Otten, L. 1996. Characterization and distribution of tartrate utilization genes in the grapevine pathogen Agrobacterium vitis. Mol. Plant-Microbe Interact. 9:401-408.

Schroth, M.N., McCain, A.H., Foott, J.H. and Huisman, O.C. 1988. Reduction in yield and vigor of grapevine caused by crown gall disease. Plant Dis. 72:241-246.

Seifi, H. S., Van Bockhaven, J., Angenon, G. and Hŏfte, M. 2013. Glutamate metabolism in plant disease and defense: Friend or foe? Mol. Plant Microbe Interat. 26: 475-485.

Smits, S., Mueller, A., Schmit, L. and Grieshaber, M.K. 2008. A structural basis for substrate selectivity and stereoselectivity in octopine dehydrogenase from *Pecten maximus*. *J. Mol. Biol.* 381:200-211.

Stover, E.W., Swartz, H.J. and Burr, T.J. 1997. Crown gall formation in a diverse collection of *Vitis* genotypes inoculated with *Agrobacterium vitis*. Am. J. Enol. Vitic. 48:26-32.

Süle, S. and Burr, T.J. 1998. The effect of resistance of rootstocks to crown gall (*Agrobacterium spp*.) on the susceptibility of scions in grapevine cultivars. Plant Pathol. 47:84-88.

Süle, S., Mozsar, J. and Burr, T.J. 1994. Crown gall resistance of *Vitis* spp. and grapevine rootstocks. Phytopathol. 84:607-611.

Szegedi, E., Korbuly, J. and Koleda, I. 1984. Crown gall resistance in East-Asian *Vitis* species and in their *V. vinifera* hybrids. Vitis 23:21-26.

Van den Berg, R., Hoefsloot, H.C.J., Westerhuis, J.A., Smilde, A.K. and Van der Werf, M.J. 2006. Centering, scaling, and transformations: improving the biological information content of metabolomics data. BMC Genomics 7:142-157.

Wallis, C. M., and Chen, J. 2012. Grapevine phenolic compounds in xylem sap and tissues are significantly altered during infection by *Xylella fastidiosa*. Phytopathol. 102:816-826.

Wallis, C. M., Wallingford, A. K. and Chen, J. 2013. Effects of cultivar, phenology, and *Xylella fastidiosa* infection on grapevine xylem sap and tissue phenolic content. Physiol. Mol. Plant Pathol. 84: 28-35.

Warren, C.R. 2013. Use of chemical ionization for GC-MS metabolite profiling. Metabolomics 9: S110-S120.

Wasson, A. P., Pellerone, F. I. and Mathesius, U. 2006. Silencing the flavonoid pathway in *Medicago truncatula* inhibits root nodule formation and prevents auxin transport

regulation by rhizobia. Plant Cell 18:1617-1629.

Wasson, A. P., Ramsay, K., Jones, M. G. K. and Mathesius, U. 2009. Differing requirements for flavonoids during the formation of lateral roots, nodules and root knot nematode galls in *Medicago truncatula.* New Phytol. 183: 167–179.

Westerhuis, J.A., Van Velzen, E.J.J., Hoefsloot, H.C. and Smilde, A.K. 2010. Multivariate paired data analysis: multilevel PLSDA versus OPLSDA. Metabolomics 6:119-128.

Wold, S., Sjöström̈a, M. and Eriksson, L. 2001. PLS-regression: a basic tool of chemometrics. Chemom. Intell. Lab. Syst. 58: 109–130

Zauner, S., Creasap, J.E., Burr, T.J. and Ullrich, C.I. 2006. Inhibition of crown gall induction by *Agrobacterium vitis* strain F2/5 in grapevine and *Ricinus*. Vitis 45:131-139.

Chapter 3

Metadata analysis of GC-MS metabolite profiling in grapevines infected with *Pseudocercospora vitis* and *Agrobacterium vitis*.

ABSTRACTS

In this experiment, metabolite profiling analyzed by GC-MS and multivariate statistical analyses was compared between the leaf tissues infected with *Pseudocercospora vitis* {including different areas such as the necrotic lesion (A), halo (B), the periphery of the lesion (C) and distant area from the lesion (D)} and healthy non-infected leaf tissues for the grapevine leaf spot, and between the internode tissues of the resistant (RR), moderately resistant (SR) and susceptible (SS) grapevines inoculated with *Agrobacterium vitis* and with wounding alone for the crown gall at the same intervals of days after inoculation {post-1; 2 days after inoculation (DAI), post-2; 7 DAI, and post-3; 30 DAI}. The raw spectrum of GC-MS revealed more numerous and intense peaks for the infected leaf tissues compared to the healthy leaf tissue, and their multivariate statistical analysis showed the most numerous metabolites including aspartic acid, maltotriose, caffeic acid and catechin occurred at the periphery of the necrotic lesion, indicating the plant-pathogen interactions were most active for disease development on this site. A total of six metabolites were identified from the comparison of the metabolite profiling between infected and healthy leaf tissues, including maltotriose, glucoheptonic acid and tartronic acid, a phenolic compound 1-hydroxyanthraquinone and two amino acids aspartic acid and L-threonine, without significant differences in their contents among different areas relative to the necrotic lesion. This suggests these may be the disease-related metabolites occurring widely around the infection sites. For the crown gall, most numerous metabolites related to the

infection or wounding significantly occurred at post-1 (8 for infection in SS, 4 for wounding in RR), second-most at post-2 (3 for infection in SS, 6 and 1 for wounding in SS and RR, respectively), and least at post-3 (all 3 for infection in RR or SR), suggesting that the responses to the pathogen infection mostly occur in the susceptible grapevines at post-1, wound healing responses occur earlier in the resistant plants than in the susceptible plants, and that no more responses to wounding occur at post-3. Based on the metabolite contents significantly increased in grapevines with different types of responses and at the period of time after inoculation and wounding, all of the results suggest that plant resistance and wound healing responses are inter-related, enhancing the other responses to increase resistance to the pathogen infection and to speed up the wound healing processes.

INTRODUCTION

In general, necrotrophic pathogens inducing necrotic symptoms destroy host plant cells and feed on the remains; however, necrotrophic or biotrophic pathogens causing hyperplastic symptoms make specific tissues that help their feeding on host nutrients (Glazebrook, 2005). Their disease development strategies and host response are quite different from each other. Representative necrotrophic fungi such as *Botrytis cinerea* and *Alternaria brassicicola* produce a variety of toxins at the very early stages of infection which promote host cell death, for which the necrotic fungal pathogens seize carbon and nitrogen sources from plant cells damaged by the toxins (Colmenares et al., 2002; MacKinnon et al., 1999). Jasmonic acid-isoleucine conjugate (JA-Ile) and ethylene (ET) are important materials as signaling molecules for resistance to the necrotic pathogens (Glazebrook, 2005). Contrastingly, a typical hyperplastic-symptoms-inducing pathogen, *Agrobacterium vitis*, make a gall tissue on the trunk and cane by transferring its DNA fragments containing a phytohormone synthesis gene set to host genome, for which factors are controlled all of these pathogenetic processes (Burr and Otten, 1999; MacKinnon et al., 1999).

Metabolite profiling has been a useful tool to elucidate the disease development and defense responses in plants; the levels of the whole plant metabolites increase or decrease at the time of pathogen infection. When *A. brassicicola* infects *Arabidopsis* plants, levels of several amino acids such as alanine, glycine, leucine, glutamic acid, and lysine are increased in responses to the pathogen infection (Botanga et al., 2012). Putrescine and stigmasterol are also increased in

responses to *A. brassicicola* as did the non-protein amino acid GABA and the disaccharide trehalose (Ward et al. 2010). In a previous study, the infection of *Hyaloperonospora arbidopsidis* in *Arabidopsis* perturbs amino acid homeostasis, leading to over-accumulation of the Asp-derived amino acids, methionine, threonine, and isoleucine (Stuttmann et al., 2011). In grapevine, at two months post inoculation with *Xylella fastidiosa*, catechin, digalloylquinic acid, and astringin were found at greater levels in xylem sap; multiple catechins, procyanidins, and stilbenoids were found at greater levels in xylem tissues; and precursors to lignin and condensed tannins were found at greater levels in xylem cell walls (Wallis and Chen, 2012). Metabolite production is influenced by *Botrytis cinerea* infection in grapevine cv. Chardonnay, resulting in the production of proline, glutamate, arginine, and alanine at significantly higher levels in the infected tissues. Moreover, degraded phenylpropanoids, flavonoid compounds, and sucrose together with markedly produced glycerol, gluconic acid and succinate are all directly associated with *B. cinerea* infection (Hong et al., 2012).

In this chapter, metabolite profiling analyzed by GC-MS in grapevine tissues is to be compared between the peripheries around infection sites of the fungal and bacterial pathogens (*Pseudocercospora vitis* and *Agrobacterium vitis*) and the wounding sites without pathogen inoculation to find out disease-related metabolites and their biological implications in the different pathosystems.

MATERIALS AND METHODS

I. Plant materials

For the leaf spot caused by *P. vitis*, grapevine 'Campbell Early' leaves showing the typical leaf spot symptoms were collected in the experimental vineyard in Suwon, Korea at harvest season in 2014. Leaf surface was cleansed with an ethanol-soaked paper towel to remove dust and debris from the surface. Leaf tissues infected with *P. vitis* were divided into four different sites; necrotic lesion area (A), halo area around A (B), the periphery area around B (C) and the healthy-looking leaf area distant from the necrotic lesion (D). Healthy-looking leaves without leaf spot symptoms were also collected from the vineyard at the same time of the harvest season. For the crown gall caused by *A. vitis*, 11~22 green shoot cuttings of 10 grapevine cultivars (*Vitis spp.*) were collected from the fields of the National Clonal Germplasm Repository (NCGR; USDA-ARS, Davis, CA, USA) in June 2015 and placed in a perlite bed for rooting at 25°C with mist for one month. For inoculation, a wound (about 1.0 mm deep) was made in the internode of the green shoot using a 2-mm-d drill and 10 μl of the bacterial suspension or distilled water (mock inoculation, control) were injected into the wound using a micropipette. After inoculation, the wound (inoculation) site was immediately wrapped with sealing film (Parafilm, WI, USA) and the green shoot cuttings were grown at 25°C in a greenhouse. Inoculated or control grapevine internode tissues were collected at the two, seven, and 30 days after wounding and inoculation, designated by post-1, post-2, and post-3, respectively.

II. GC-MS analysis and multivariate data analysis

GC-MS metabolites profiling followed the method of previous reports (Kim et al., 2015, and Jung et al., 2016). Acquired data were analyzed using the multivariate analysis methods (Eriksson, 2006, and Westerhuis et al., 2009) as described in Chapter 1 and Chapter 2. In this Chapter, however, the metabolite profiling of the healthy leaf tissues with mock inoculation (wounding alone) was compared with those of the tissues with the pathogen inoculation, including the viable leaf areas of B~D for the leaf spot and at the same period of time after wounding (inoculation) (at post-1, post-2 and post-3) for the crown gall, respectively. Metabolites related to the pathogen infection, healthy leaf or mock inoculation were analyzed using a correlation coefficient table and box plot for comparing with those of the previous results described in Chapter 1 and Chapter 2.

RESULTS AND DISCUSSION

I. Leaf spot caused by *P. vitis*.

GC-MS metabolic profiling is one of the methods for identifying whole metabolites. In this experiment, the whole metabolites revealed in the raw spectrum of GC-MS for the leaf tissues of peripheral area (B) around leaf spot symptoms (necrotic lesion) and healthy leaf tissues largely showed general differential features, revealing more numerous and intense peaks for the infected leaf tissues compared to the healthy leaf tissue (Fig. 3-1). However, this brought up a little information on specific metabolites that could be clearly differentiated from the other state of leaf tissues either diseased or healthy, for which statistical analysis should be conducted to reveal significantly critical metabolites related to the development of the leaf spot with either positive or negative value.

Multivariate statistical analysis of the metabolic components identified by GC-MS in the grapevine leaf tissues with and without the pathogen infection showed metabolite compositions in the non-infected healthy leaf tissues were significantly different from those in the halo around the necrotic lesion (B), adjacent peripheral area (C) and even distant area that showed little influence of the disease (D); however, there were no critical differences in the chemical compositions among the areas in the same leaves infected with the pathogen (Table 3-1). This suggests the healthy-looking leaf tissues distant from the leaf spot symptoms may not be free of the influence of the pathogen infection so that the pathogen infection in a small portion of the leaf tissue may affect the metabolism of leaf tissues in a wide area around the original infection

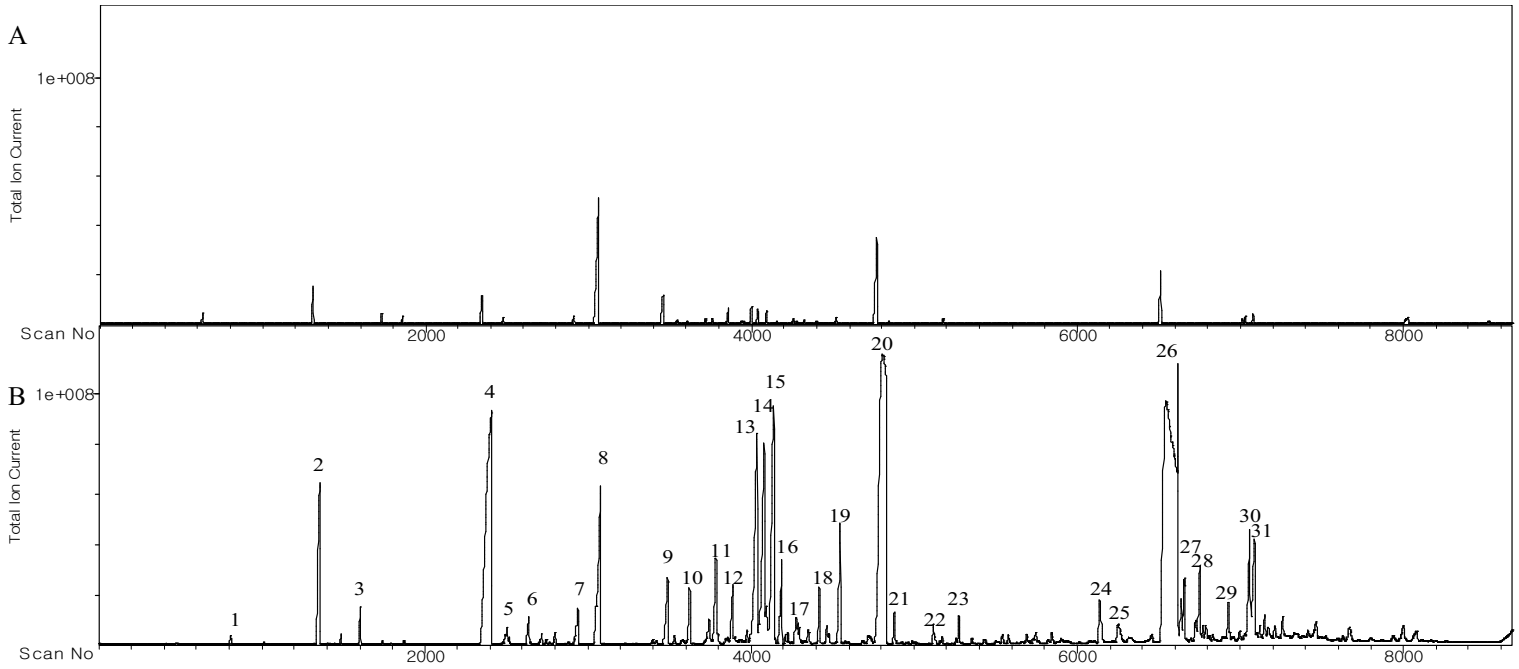

Figure 3-1. GC spectrums of noninvasive leaf tissue (N) and the periphery of symptom caused by *Pseudocercospora vitis* (B) in grapevine cv. 'Campbell Early'. Metabolites list, 1: 1-hydroxyanthraquinone, 2: phosphoric acid, 3: glyceric acid, 4: malic acid, 5: L-glutamic acid, 6: tartronic acid, 7: L-glutamic acid, 8: tartaric acid, 9: purine riboside, 10: lactulose, 11: citric acid, 12: dehydroascorbic acid, 13, 14: fructose, 15: glucose, 16: D-allose, 17: galacturonic acid, 18: galactinol, 19: gluconic acid, 20: myo-inositol, 21: caffeic acid, 22: maltotriose, 23: methyl-beta-D-galactropyranoside, 24, 25: lactose, 26: sucrose, 27: resveratrol, 28, 29: melezitose, 30: epicatechin, 31: catechin.

Table 3-1. The correlation of disease related metabolites in OPLS-DA models between control leaf tissue and infected leaf tissue caused by *Pseudocercospora vitis*.

CAS-Number	Name	Classification	Control vs. infected leave		
			B	C	D
129-43-1	1-hydroxyanthraquinone	Phenolic compound	0.8933	0.7614	0.6670
56-84-8	Aspartic acid	Amino acid			0.5988
10094-62-9	Glucoheptonic acid	Carboxylic acid		0.8743	0.9078
72-19-5	L-threonine	Amino acid		0.8796	
1109-28-0	Maltotriose	Carbohydrate	0.6916	0.6516	0.5233
80-69-3	Tartronic acid	Carboxylic acid		0.5234	0.5098
331-39-5	Caffeic acid	Carboxylic acid	0.6321		
154-23-4	Catechin	Flavonoid		0.8820	
579-36-2	D-allose	Carbohydrate	0.6338		
490-83-5	Dehydroascorbic acid	Carboxylic acid	0.6595	0.5839	0.5689
57-48-7	Fructose	Carbohydrate	0.9426		
473-81-4	Glyceric acid	Carboxylic acid		0.8698	0.5721
56-86-0	L-glutamic acid	Amino acid		0.6693	

z. Chemical Abstracts Service registry number: American Chemistry Society

y. Sampling tissue name; B: halo of symptom, C: periphery of symptom, D: not infected tissue

sites, possibly leading to the whole leaf to be non-functional at a certain period of the pathogen infection stages to make the leaf defoliated. The degree of this spreading effect may vary depending upon the host-parasite relationships.

A total of six metabolites were identified from the comparison of the metabolite profiling between infected and healthy leaf tissues by excluding those that varied among the areas on the leaf infected with the pathogen (Table 3-1). These included one carbohydrate (maltotriose), two carboxylic acids (glucoheptonic acid and tartronic acid), one phenolic compound (1-hydroxyanthraquinone) and two amino acids (aspartic acid and L-threonine). However, there was no significant difference in these metabolite contents among the areas at different distances from the necrotic symptoms, suggesting these metabolites may not be found in the healthy leaf tissues but only in the infected leaf tissues, which may be disease-related metabolites. There are no direct or indirect evidence sufficiently illustrating the biological roles of these metabolites in the progress of disease development. However, considering the necrotrophic pathogenesis of the disease and wide distribution of the materials around the infection sites, these metabolites may be the materials released from the leaf tissues degraded by phytotoxic and enzymatic activities of the invading pathogen, possibly related to the formation of the typical necrotic spot symptoms, which resembles programmed cell death (or systemic acquired resistance response) in pathogenesis (Fu and Dong, 2013; Agrios, 2005).

There are physiological changes such as photosynthesis, respiration and nitrogen metabolism around the infection sites of plant pathogens (Agrios, 2005). The light reactions of

photosynthesis, the Calvin cycle, and the stress responses are changed in infection sites of the tan spot disease in wheat, in which the decrease of photosynthesis in the infected leaf results from ROS generation and disruptions of the photosynthetic electron transport shortly after pathogen attack (Kim et al., 2010). A decreased photosynthesis and stomatal closure are associated with the infection of esca disease (a type of grapevine trunk disease) in leaves, which is followed by the general increase of respiration rates (Petit et al., 2006). For nitrogen metabolism, aspartic acid conjugates with indole-3-acetic-acid (IAA) as a signal and promotes plant susceptibility to the pathogen; aspartic acid and threonine have a complementary relationship to the disease development in the plant cell (González-Lamothe et al., 2012). *P. vitis* causing grapevine leaf spot is a relative species of *Cercospora spp.* that has a none host-specific toxin (cercosporin) that releases singlet oxygen in response to light (Daub, 1982). When growing *P. vitis* in potato-dextrose agar, it secretes a red pigment into the medium that seems to be related to a toxin like cercosporin. When *B. cinerea* is invading in grape berry, localized H_2O_2 production and lignin synthesis are enhanced that are related to defense responses of the necrotic pathogens (Kelloniemi et al., 2015).

Figure 3-2 showed the relative abundances of metabolites in the areas of necrotic lesion, halo, the periphery of the necrotic lesion and halo, and the distant area from the necrotic lesion. Most numerous metabolites occurred in the periphery of the necrotic lesion, including a quinone derivate 1-hydroxyanthraquinone with antimicrobial activity (Wang et al., 2010) and others

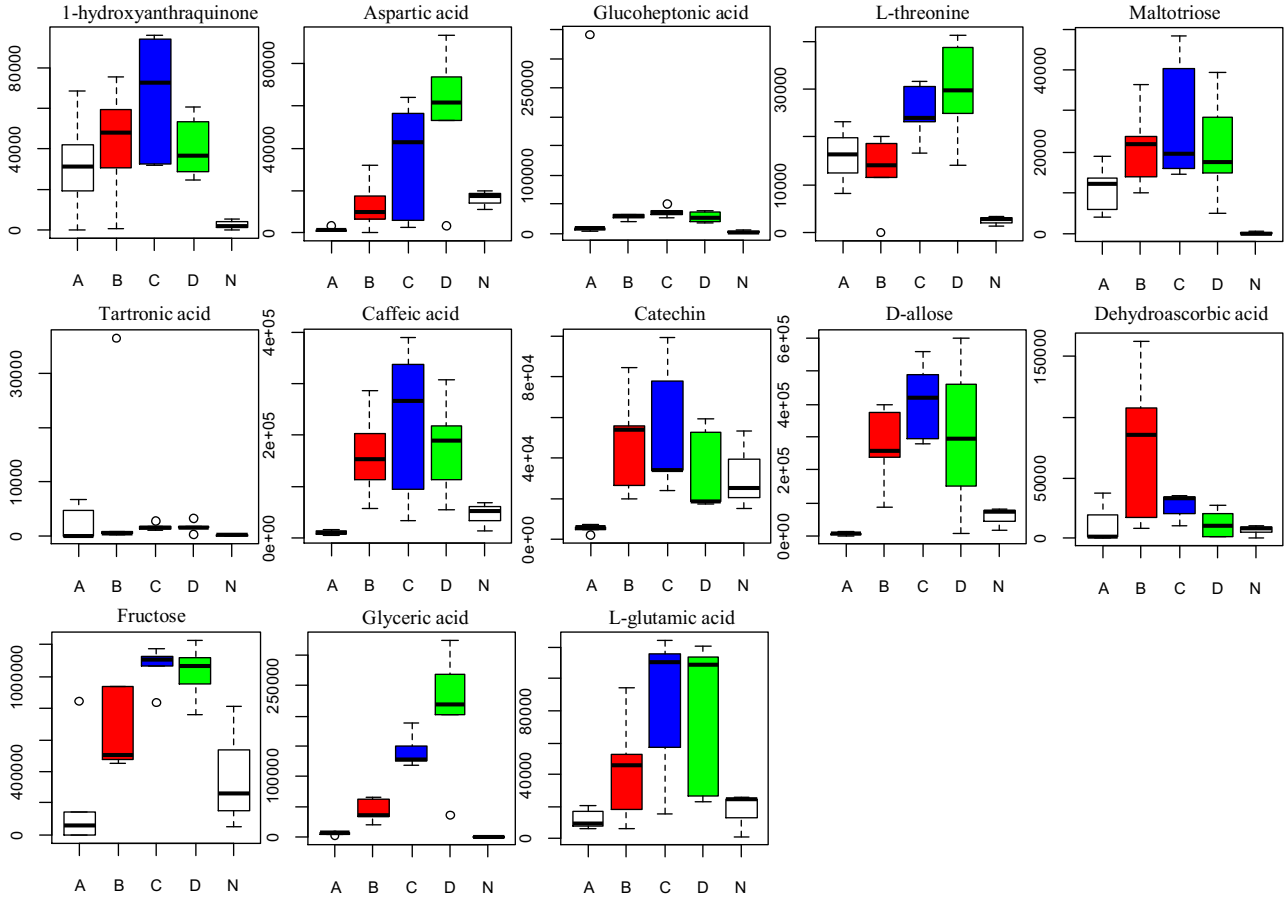

Figure 3-2. Relative abundances of metabolites in the areas of infected leaf tissues (A: necrotic lesion, B: halo, C: periphery of the necrotic lesion, D: distant area from necrotic lesion) and control healthy leaf tissue (N).

(aspartic acid, maltotriose, caffeic acid and catechin), suggesting the host-pathogen reactions may be the most active in the peripheral areas of the infection sites than other inner (halo) and distant outer area of the necrotic lesion, of which the related materials may be involved in necrotic symptom development and initial tissue degradation, respectively. All of these results suggests that metabolite profiling of the grapevine leaf tissues infected with *P. vitis* may reveal the dynamic nature of disease progression in the necrotrophic pathosystem.

II. The crown gall caused by *A. vitis*.

Little information was available about the whole dynamic metabolites changes in the host responses after *A. vitis* inoculation in grapevine internodes in Chapter 2, in which the effects of wound have not been discriminated in the inoculation test of the pathogen so that the metabolite profiling of the internode tissues might result from not only host responses to the pathogen infection but also responses to the wound (wound healing). Thus, in this experiment, GC-MS metabolite profiling of the grapevine species infected with *A. vitis* was compared with those treated with distilled water (wound alone) at the same intervals of days after wounding and inoculation (DAI).

Comparison of the metabolite profiling showing the metabolite contents related to the crown gall disease varied depending on the infection stages and host response types (Table 3-2; Fig. 3-3, 3-4). Totally, most numerous metabolite contents were related either to the disease or Table

Table 3-2. The correlation of disease related metabolites in OPLS-DA models between *A. vitis* and distilled water inoculation.

Stage	Name	RR		SR		SS	
		A. vitis	D.W.	*A. vitis*	D.W.	*A. vitis*	D.W.
Pre	Cellobiose	0.5326					
Post-1 (2DAI)	Asparagine					0.5904	
	Gallocatechin					0.5245	
	Cellobiose					0.5376	
	Glutamine					0.7082	
	Histidine					0.7366	
	Resveratrol	0.5799					
	Sucrose	0.5493		0.5137			
	Tyrosine					0.6320	
	beta-sitosterol		0.6103				
	Putrescine		0.5669				
	Tartaric acid		0.7461				
	Trehalose		0.6261				
Post-2 (7DAI)	Cellobiose					0.5527	
	Gallocatechin					0.6864	
	Quinic acid					0.5747	
	Alanine						0.5383
	Epicatechin						0.7923
	Galactinol						0.6476
	Gallocatechin						0.6046
	Isocitric acid		0.5847				
	Maltose						0.8160
	Raffinose		0.5094				
	Tryptophan						0.5885
Post-3 (30DAI)	Sucrose			0.6342			
	Valine	0.7367					
	Xylonic acid	0.5903					

wounding at post-1 (12 metabolites), second-most at post-2 (11 metabolites), and least at post-3 (3 metabolites); most numerous in the grapevine species with a response type of SS (16 metabolites), second-most in RR (11 metabolites), and least in SR (2 metabolites), which is largely coincided with the results shown in Chapter 2 that the disease-related metabolites were compared with those of pre-inoculation stage as control. At post-1, 8 metabolites were related to the disease, 4 related to wound; at post-2, 3 related to the disease, 8 related to wound; and at post-3, all three related to the disease, but non-related to wound, indicating the prevailing responses were initially against the pathogen infection, intermittently to wound healing, and lately to disease development.

At post-1 (2 DAI), amino acids such as asparagine, glutamine, histidine, and tyrosine were related to the disease in the response type of SS. These amino acids increased during the pathogen infection may be due to the increased apoplastic protease activity of several proteases induced in grapevine tissues by the pathogen infection (Dulermo et al., 2009). In *Agrobacterium spp*, *VirH2* detoxifies wound-released plant phenolics by catabolism, mineralization or conversion into sources of carbon, energy or nutrients (Brencic et al., 2004). At post-1, there was no metabolite significantly related to the disease in the grapevines of RR, in which contents of β-sitosterol, putrescine, tartaric acid, and trehalose were relatively higher (related more to wound) than in SR and SS (Table 3-2; Figure 3-3), suggesting that wound healing responses may be more active in the resistant grapevines than the susceptible ones. β-sitosterol is a phytosterol which is related to disease resistance of *Arabidopsis* after pathogen attack

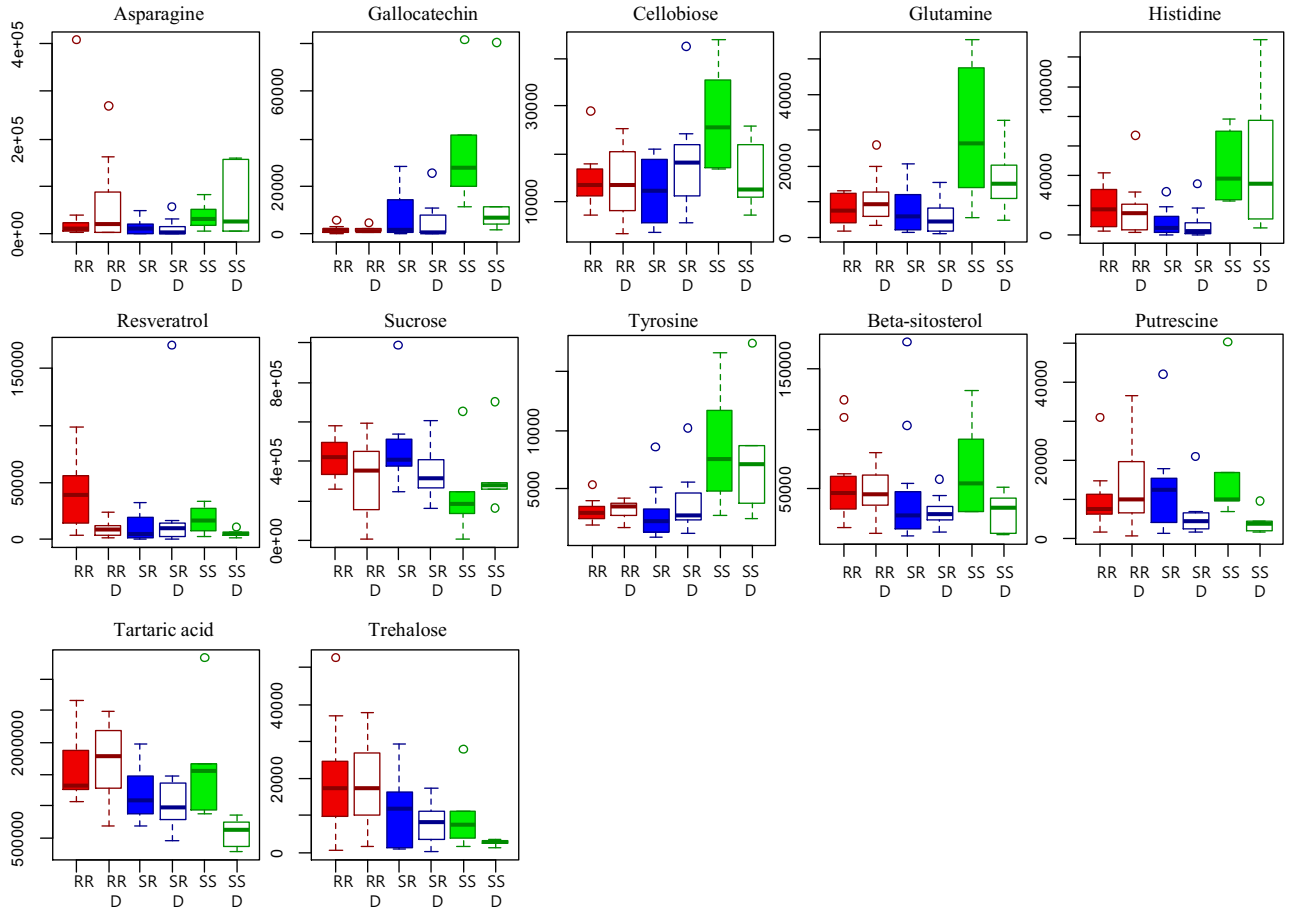

Figure 3-3. Relative abundances of metabolites in internode tissues of grape species of response types of RR (red), SR (blue) and SS (green) inoculated with *A.vitis* (solid box) and treated with distilled water as control (blank box) at the post-1 stage.

(Griebel and Zeier, 2010). Stigmasterol in *Arabidopsis* is produced to saturate *β*-sitosterol. The induced accumulation of leaf stigmasterol and an overall increase in the ratio of stigmasterol to *β*-sitosterol in leaves favour apoplastic *P. syringae* multiplication, leading to the enhancement of disease susceptibility, which implies that there is no conversion of *β*-sitosterol to other forms of sterols in the leaf tissues wounded. Putrescine, one of the polyamines, is regulated by mitogen-activated protein kinase (MAPK) cascade in *Arabidopsis* as stress responses (Kim et al., 2013). Putrescine synthesis starts from arginine using arginine decarboxylase (ADC). ADCs are activated under abiotic stresses such as wound and cold, and salt stress (Hussain et al., 2011). Several cases have been reported that putrescine synthesis pathway is related to biotic stresses from pathogens such as fungi (Greenland and Lewis, 1984), virus (Uehara et al., 2005), and bacteria (Takahashi, 2016). However, polyamines are used for various regulation parts of environmental adaptation, development, and biochemical changes in the plant (Hussain et al., 2011). When mechanical wounds are made of the plant tissues, phenylalanine ammonia-lyase (PAL) starts phenylpropanoid metabolism in 36 hours after wounding for the wound healing (Campos et al., 2004). Tartaric acid is a major carboxylic acid in grape and commonly detected in most grape tissues, and thus, its increase in the grapevine internode tissue after wounding might not be unusual aspects to happen at the early stage of the pathogen infection (at post-1). However, the content of tartaric acid differed among response types, showing the highest in RR than other response types, suggesting wound healing processes may be activated rapidly at early stages after wounding in the grapevine tissues with RR. Trehalose is a powerful sugar signal in

plant metabolic pathway (Paul et al., 2008). It is disaccharide which induces resistance to powdery mildew in wheat (Reignault et al., 2001). However, no specific function for trehalose in plant-microbe interactions has so far been clearly identified together with trehalose and tre6P in plant responses to abiotic stresses (Figueroa and Lunn, 2016).

The reaction in the post-1 stage after wounding is the initial response to healing the wound. Wound healing response initiate inter- and intra- cellular sensing at the early stage which activates defense response. Late responses such as deposition of callose, suberin, lignin and synthesis of various phenolics that may function both as a physical barrier and as antimicrobial substances (Savatin et al., 2014). In previous studies on gene expression, disease, and stress-related genes show similar and overlapping expression levels in the wounding and pathogen inoculation (Ditt et al., 2006; Lee et al., 2009; Deeken et al., 2006; Choi and Yun, 2016). Unlike the tests on the gene expression, the same metabolites did not appear between *A. vitis* inoculation and wounding alone. In the post-1 stage, specific metabolites in wounding alone were significantly different among the different groups, especially in the RR group, which was significantly higher than the SS group. Although the difference of metabolite content is very small, unlike the SS and SR groups, they have a high content in the RR group (Figure. 3-3). It understands that inhibition of ROS response by *A. vitis* (Lee et al., 2009) does not occur in the SS group, and wound healing process occurs in the RR group.

At post-2 (one week after wounding and inoculation), more metabolites, which mostly occurred in SS, were related to the wound than those related to the disease at the same stage and than

those related to wound at post-1, suggesting the host responses to the wound have been retarded and complicated in the grapevine internode tissues susceptible to *A. vitis*, probably because of the tissue degradation caused by the pathogen infection that may hinder wound healing. The wound-related metabolites were alanine, epicatechin, galactinol, gallocatechin, maltose, and tryptophan in SS, but isocitric acid and raffinose in RR (Figure 3-4). The reduction of metabolites in RR indicates the completion of the wound healing processes for which no further wound responses are required. In a previous report, metabolite profiling in *Arabidopsis* also reveals that several amino acids such as valine, leucine, and tyrosine accumulate after treatment with avirulent and virulent pathogens (Rojas et al., 2014). In general, under the attack of a pathogen, plants alert their induced defense mechanisms, for which amino acids are involved in numerous fundamental metabolic pathways including disease resistance in the plant (Agrios, 2005). Tryptophan is an aromatic amino acid and a major precursor for multifunctional indole compounds (Tzin and Galili, 2010). These all suggest the resistance responses against *A. vitis* may be triggered by the responses to wound, which may be activated as rapid wound healing processes in RR. The bacterial pathogen, *A. vitis*, generally penetrates grapevine stems through wounds and its disease development (gall development) in the grapevines is enhanced by the wounding which increases phenolic acids and acidic monosaccharides released from the cell vacuoles, which induce the expression of *vir* gene family for its pathogenesis (Agrios, 2005; Ankenbauer and Nester, 1990; Douglas, 1996; Stachel et al., 1986). However, various plant species and plant organs differ in their responses to usually wounding by forming boundary

layers (wound periderms) and deposition of cell walls fortification materials such as lignin and suberin to inhibit the disease development (Chang et al., 2016; Rittinger et al., 1986). The infectivity of the fungal pathogen, *Colletotrichum acutatum*, is reduced by the delayed inoculation of the pathogen after wounding, in which the formation of wound periderm as wound healing processes is enhanced to block the pathogen invasion (Kim et at., 2008). Also, the wound healing process occurs rapidly in the peach trees resistant to *Botryosphaeria* sp., which is indicated by the rapid wound periderm formation, compared to the trees susceptible to the fungal pathogen (Biggs and Stobbs, 1986). These suggest the rapid wound responses may prevent the penetration and invasion of plant pathogens, and the metabolites produced as responses to wounding in the resistant grapevines can be used for resistant responses against the bacterial infection. In the case of raffinose, the difference was not significant among the RR, SR, and SS groups with *A. vitis* inoculation, but the SS group had a significantly higher amount of raffinose in grapevines with the pathogen inoculation than with wounding alone. However, it seems to be an additional result that raffinose is sharing the same substrate with for the synthesis of galactinol. Also, raffinose has lower contents than RR and SR group in SS group and is considered to be related to disease development as in galactinol. The difference in galactinol content between the groups in the distilled water treatment is evidence that the response to osmotic stress caused by the wound in the plant is an important disease development in crown gall disease. Galactinol and raffinose are closely related each other; galactinol is synthesized from sucrose by the activity of galactinol synthases, and then conjugated with sucrose to

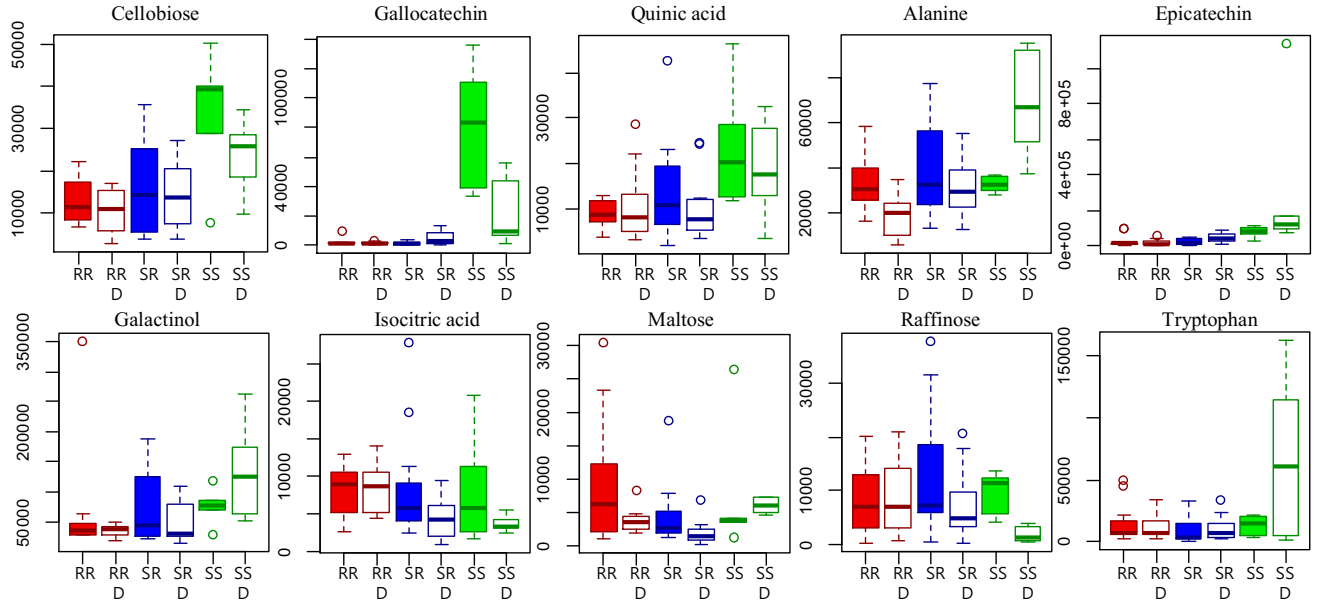

Figure 3-4. Relative abundances of metabolites in internode stem tissues of grape species of response types of RR (red), SR (blue) and SS (green) inoculated with *A. vitis* (solid box) and treatment with distilled water as a control (blank box) at the post-2 stage.

produce raffinose (Nishizawa et al., 2008). Galactinol and raffinose accumulate in the intracellular space in responses to environmental stresses. In *Arabidopsis*, the transcription levels of galactinol synthases are increased under the salinity and drought stresses, and the overexpression of galactinol synthase in *Arabidopsis* plants shows increased tolerance to the drought stress (Taji et al., 2002). Galactinol and raffinose act as osmoprotectants and ROS-scavenger to reduce oxidative damages caused by salinity, chilling and drought (Nishizawa et al., 2008), suggesting these two materials may play a role in defense responses against the pathogen infection, although their principal roles are the protection of the plants from several abiotic stresses as mentioned above. Maltose is a disaccharide, which is converted to glucose, fructose, and sucrose in the cytosol of the cell is closely related to the responses against environmental stresses including wound (Krasensky and Jonak, 2012). However, the content of maltose is increased, accompanying the decrease of starch, by abscisic acid treatment and under salt stresses, suggesting it may rather be a product resulting from the stressful conditions than a reactant involved in the active response for wound healing.

Gallocatechin was a common metabolite significantly related to the disease at post-1 and the wound at post-2 in SS for all (Table 3-2). The amount of gallocatechin in the SS group was increased in the *A.vitis* inoculation and wound treatment at the different time. It seems that gallocatechin is not directly related to the disease development but continuously responded stress against wounding. Gallocatechin is a related to plant responses to various kinds of outer stress such as UV radiation, temperature, drought, *etc* (Mierziak et al., 2014). Gallocatechin is a

flavan-3-ol and one of the antioxidant chemical. Gallocatechin intercalates into phospholipid bilayers, and it is likely that it affects on both virulence and antibiotic resistance by perturbing the function of key processes associated with the bacterial cytoplasmic membrane (Taylor et al., 2005). This molecule has the capacity of modulating the physical structure of cell membranes; and above all, its primary activities (together with epicatechin) in the plant reveal antioxidation and scavenging capacities that differ in activity levels according to its structure (Pietta, 2000), suggesting this phenolic compound may be closely related to defenses against biotic and abiotic stresses as well.

Another phenolic compound, resveratrol, was significantly increased in RR at the initial stages of the pathogen infection (at post-1), but neither in RR with wounding alone nor in SS and at later stages of infection regardless of pathogen inoculation and wounding alone, suggesting this metabolite may be related to the resistance response to *A. vitis*, which may be free of the influences from wounding as was noticed in Chapter 2. In his experiment, isocitric acid was only related to the wound in RR at post-2. Isocitric acid is an organic acid closely related to citric acid, which is relatively increased in content under a salt stress, compared to salt stress-free conditions (Muscolo et al., 2015). This suggests that isocitric acid may be involved in wound healing processes at an advanced stage after wounding or may be a product occurring during the wound healing processes.

At post-3, only three metabolites occurred significantly in responses to the pathogen

infection in the grapevines with RR or SR, but no metabolite was detected in response to wounding. This suggests the degrees of disease responses lowered much compared to those in the previous stages, and the wound healing responses were completed by this stage after wounding.

In plant tissues, reactive oxygen species (ROS) are common mechanism inducing programmed cell death (PCD), which is related to hypersensitive responses (HR) as resistance responses and wound healing processes as well (Angelini et al., 2008). Among a variety of ROS, hydrogen peroxide (H_2O_2) is involved in response to mechanical damage which also related to plant defense response necessarily. Polyamine-derived H_2O_2 is involved in cell wall differentiation by driving peroxidase-mediated oxidative cross-linking of cell wall components or behaves like the second messenger in signaling programmed cell death (PCD) (Tisi et al., 2008). Hydrogen peroxide is detected within 1 h after wounding and increase 4~6 h both locally and systemic other unwounded tomato plant parts (Savatin et al., 2014). At the early infection stage of *A. tumefacience* in *Arabidopsis*, agrobacteria can suppress H_2O_2 accumulation for retaining gall development (Lee et al., 2009). Wound healing includes the deposition of suberin on the cell wall, and fortification of cell wall structure with polyphenolic compounds but it is relatively later than the chemical responses mentioned above (Sherf et al., 1993),.

In this experiment, the pathogen inoculation was conducted through the wound made at the same time of the inoculation, which implies wound healing responses may proceed the defense

response against the pathogen infection. Considering the similarities of defense and wound healing responses in regards to PCD and fortification of cell wall structure, the wound healing responses before responses to the pathogen infection may enhance resistance responses of the grapevines with RR to the pathogen infection. Conversely, wound healing processes are enhanced in resistant plants inoculated with avirulent pathogens, compared to wounding alone (Kim and Kim, 2002; Kim et al., 2004). It suggests that the wound healing may be enhanced in the resistant plants by the inoculation of avirulent pathogen strains. For susceptible plants, however, wound healing processes were retarded until the disease development, indicated by the later increase of wound-related metabolites in this experiment, and the pathogen's invasion might be in an active progression without the structural defenses derived from the wound healing responses. All of these aspects related to pathogen infection and wounding revealed by metabolite profiling would provide valuable information and new insights on the understandings of the diseases so as to be used for the development of grapevine disease management strategies.

LITERATURE CITED

Agrios, J., N., 2005. Plant Pathology, in: Plant Pathology (Fifth Edition). Academic Press, San Diego

Angelini, R., Tisi, A., Rea, G., Chen, M.M., Botta, M., Federico, R., Cona, A., 2008. Involvement of polyamine oxidase in wound healing. Plant Physiol. 146: 162–177.

Biggs, A.R., and Stobbs, L.W. 1986. Fine structure of the suberized cell walls in the boundary zone and necrophylatic periderm in wounded peach bark. Can. J. Bot. 64:1606-1610.

Botanga, C.J., Bethke, G., Chen, Z., Gallie, D.R., Fiehn, O., Glazebrook, J., 2012. Metabolite profiling of *Arabidopsis* inoculated with *Alternaria brassicicola* reveals that ascorbate reduces disease severity. Mol. Plant. Microbe Interact. 25: 1628–1638.

Brotman, Y., Lisec, J., Meret, M., Chet, I., Willmitzer, L., Viterbo, A., 2012. Transcript and metabolite analysis of the *Trichoderma*-induced systemic resistance response to *Pseudomonas syringae* in *Arabidopsis thaliana*. Microbiology 158: 139–146.

Burr, T.J., Otten, L., 1999. Crown gall fo grape: biology and disease management. Annu. Rev. Phytopathol. 37: 53–80.

Colmenares, A.J., Aleu, J., Durán-Patrón, R., Collado, I.G., Hernández-Galán, R., 2002. The putative role of botrydial and related metabolites in the infection mechanism of *Botrytis cinerea*. J. Chem. Ecol. 28: 997–1005.

Campos, R., Nonogaki, H., Suslow, T., Saltveit, M.E., 2004. Isolation and characterization of a wound inducible phenylalanine ammonia-lyase gene (*LsPAL1*) from romaine lettuce

leaves. Physiol. Plant. 121: 429–438.

Daub, M.E., 1982. Cercosporin, a photosensitizing toxin from *Cercospora* species. Phytopathol. 72: 370-374.

Dulermo, T., Bligny, R., Gout, E., Cotton, P., 2009. Amino acid changes during sunflower infection by the necrotrophic fungus *B. cinerea*. Plant Signal. Behav. 4: 859–861.

Figueroa, C.M., Lunn, J.E., 2016. A tale of two sugars - trehalose 6-phosphate and sucrose. Plant Physiol. pp.00417.

Fu, Z.Q., Dong, X., 2013. Systemic acquired resistance: turning local infection into global defense. Annu. Rev. Plant Biol. 64: 839–863.

Glazebrook, J., 2005. Contrasting mechanisms of defense against biotrophic and necrotrophic pathogens. Annu. Rev. Phytopathol. 43: 205–227.

González-Lamothe, R., Oirdi, M.E., Brisson, N., Bouarab, K., 2012. The conjugated auxin indole-3-acetic acid–aspartic acid promotes plant disease development. Plant Cell 24:762-777.

Greenland, A.J., Lewis, D.H., 1984. Amines in barley leaves infected by brown rust and their possible relevance to formation of “Green Islands.” New Phytol. 96: 283–291.

Griebel, T., Zeier, J., 2010. A role for β-sitosterol to stigmasterol conversion in plant-pathogen interactions: stigmasterol promotes plant susceptibility. Plant J. 63: 254–268.

Hong, Y.-S., Martinez, A., Liger-Belair, G., Jeandet, P., Nuzillard, J.-M., Cilindre, C., 2012. Metabolomics reveals simultaneous influences of plant defence system and fungal

growth in *Botrytis cinerea*-infected *Vitis vinifera* cv. Chardonnay berries. J. Exp. Bot. 63: 5773–5785.

Hussain, S.S., Ali, M., Ahmad, M., Siddique, K.H.M., 2011. Polyamines: natural and engineered abiotic and biotic stress tolerance in plants. Biotechnol. Adv. 29: 300–311.

Jung, S.M., Hur, Y.Y., Preece, J.E., Fiehn, O., Kim, Y.H., 2016. Profiling of disease-related metabolites in grapevine internode tissues infected with *Agrobacterium vitis*. Plant Pathol. J. 32: 489–499.

Kelloniemi, J., Trouvelot, S., Héloir, M.-C., Simon, A., Dalmais, B., Frettinger, P., Cimerman, A., Fermaud, M., Roudet, J., Baulande, S., Bruel, C., Choquer, M., Couvelard, L., Duthieuw, M., Ferrarini, A., Flors, V., Le Pêcheur, P., Loisel, E., Morgant, G., Poussereau, N., Pradier, J.-M., Rascle, C., Trdá, L., Poinssot, B., Viaud, M., 2015. Analysis of the molecular dialogue between gray mold (*Botrytis cinerea*) and Grapevine (*Vitis vinifera*) reveals a clear shift in defense mechanisms during berry ripening. Mol. Plant. Microbe Interact. 28: 1167–1180.

Kim, K.H., Yoon, J.B., Park, H.G., Park, E.W., Kim, Y.H. 2004. Structural modifications and programmed cell death of chili papper fruit related to resistance response to *Colletotrichum gloeosporioides* infection. Phytopathol. 94:1295-1304.

Kim, S.G., Kim, Y.H., Kim, H.T. and Kim, Y. H. 2008. Effect of delayed inoculation after wounding on the development of Anthracnose disease caused by *Colletotricum acutatum* on chill papper fruit. Plant Pathol. J. 24: 392-399.

Kim, S.H., Kim, S.H., Yoo, S.J., Min, K.H., Nam, S.H., Cho, B.H., Yang, K.Y., 2013. Putrescine regulating by stress-responsive MAPK cascade contributes to bacterial pathogen defense in *Arabidopsis*. Biochem. Biophys. Res. Commun. 437: 502–508.

Kim, S.J., Jeong, S.H., Hur, Y.Y., Jung, S.M., 2015. Metabolite profiling of four different tissue locations in grape leaf of brown spot disease caused by *Pseudocercospora vitis*. Plant Omics 8: 523-528.

Kim, Y. H., Kim, K. H. 2002. Abscission layer formation as a resistance response of Peruvian apple cactus against *Glomerella cingulate*. Phytopathol. 92: 964-969.

Kim, Y.M., Bouras, N., Kav, N.N.V., Strelkov, S.E., 2010. Inhibition of photosynthesis and modification of the wheat leaf proteome by Ptr ToxB: A host-specific toxin from the fungal pathogen *Pyrenophora tritici-repentis*. Proteomics 10: 2911-2926.

Krasensky, J., Jonak, C., 2012. Drought, salt, and temperature stress-induced metabolic rearrangements and regulatory networks. J. Exp. Bot. err460.

Lee, C.W., Efetova, M., Engelmann, J.C., Kramell, R., Wasternack, C., Ludwig-Muller, J., Hedrich, R., 2009. *Agrobaterium tumetaciens* promotes tumor induction by modulating pathogen defense in *Arabidopsis thaliana*. Plant Cell 21: 2948-2962.

MacKinnon, S.L., Keifer, P., Ayer, W.A., 1999. Components from the phytotoxic extract of *Alternaria brassicicola*, a black spot pathogen of canola. Phytochem. 51: 215-221.

Mierziak, J., Kostyn, K., Kulma, A., 2014. Flavonoids as important molecules of plant interactions with the Environment. Molecules 19: 16240-16265.

Muscolo, A., Junker, A., Klukas, C., Weigelt-Fischer, K., Riewe, D., Altmann, T., 2015. Phenotypic and metabolic responses to drought and salinity of four contrasting lentil accessions. J. Exp. Bot. erv208.

Nishizawa, A., Yabuta, Y., Shigeoka, S., 2008. Galactinol and raffinose constitute a novel function to protect plants from oxidative damage. Plant Physiol. 147: 1251-1263.

Paul, M.J., Primavesi, L.F., Jhurreea, D., Zhang, Y., 2008. Trehalose metabolism and signaling. Annu. Rev. Plant Biol. 59:417-441.

Petit, A.N., Vaillant, N., Boulay, M., Clément, C., Fontaine, F., 2006. Alteration of photosynthesis in grapevines affected by Esca. Phytopathol. 96: 1060-1066.

Pietta, P.G., 2000. Flavonoids as antioxidants. J. Nat. Prod. 63: 1035-1042.

Reignault, P., Cogan, A., Muchembled, J., Lounes-Hadj Sahraoui, A., Durand, R., Sancholle, M., 2001. Trehalose induces resistance to powdery mildew in wheat. New Phytol. 149: 519-529.

Rittinger, P.A., Biggs, A.R., Peirson, D.R. 1986. Histochemistry of lignin and suberin deosition in boundary layersss formed after wounding in various plant species and organs. Can. J. Bot. 65:1886-1892.

Rojas, C.M., Senthil-Kumar, M., Tzin, V., Mysore, K.S., 2014. Regulation of primary plant metabolism during plant-pathogen interactions and its contribution to plant defense. Front. Plant Sci. 5: 17.

Savatin, D.V., Gramegna, G. modesti, V., Cervone, F., 2014. Wounding in the plant tissue: the

defense of a dangerous passage. Front. Plant Sci. 5: 470.

Sherf, B.A., Bajar, A.M., Kolattukudy, P.E., 1993. Abolition of an inducible highly anionic peroxidase activity in transgenic Tomato. Plant Physiol. 101: 201-208.

Stuttmann, J., Hubberten, H.-M., Rietz, S., Kaur, J., Muskett, P., Guerois, R., Bednarek, P., Hoefgen, R., Parker, J.E., 2011. Perturbation of *Arabidopsis* amino acid metabolism causes incompatibility with the adapted biotrophic pathogen *Hyaloperonospora arabidopsidis*. Plant Cell 23: 2788-2803.

Taji, T., Ohsumi, C., Iuchi, S., Seki, M., Kasuga, M., Kobayashi, M., Yamaguchi-Shinozaki, K., Shinozaki, K., 2002. Important roles of drought- and cold-inducible genes for galactinol synthase in stress tolerance in *Arabidopsis* thaliana. Plant J. 29: 417-426.

Takahashi, Y., 2016. The role of polyamines in plant disease resistance. Environ. Control Biol. 54: 17-21.

Taylor, P.W., Hamilton-Miller, J.M.T., Stapleton, P.D., 2005. Antimicrobial properties of green tea catechins. Food Sci. Technol. Bull. 2: 71-81.

Tisi, A., Angelini, R., Cona, A., 2008. Wound healing in plants. Plant Signal. Behav. 3: 204-206.

Tzin, V., Galili, G., 2010. New Insights into the shikimate and aromatic amino acids biosynthesis pathways in plants. Mol. Plant 3: 956-972.

Uehara, Y., Takahashi, Y., Berberich, T., Miyazaki, A., Takahashi, H., Matsui, K., Ohme-Takagi, M., Saitoh, H., Terauchi, R., Kusano, T., 2005. Tobacco ZFT1, a transcriptional repressor with a *Cys2/His2* Type zinc finger motif that functions in spermine-signaling

pathway. Plant Mol. Biol. 59: 435-448.

Wallis, C.M., Chen, J., 2012. Grapevine phenolic compounds in xylem sap and tissues are significantly altered during infection by *Xylella fastidiosa*. Phytopathology 102: 816-826.

Wang, J., Zhao, H., Kong, W., Jin, C., Zhao, Y., Qu, Y., Xiao, X., 2010. Microcalorimetric assay on the antimicrobial property of five hydroxyanthraquinone derivatives in rhubarb (*Rheum palmatum* L.) to *Bifidobacterium adolescentis*. Phytomedicine Int. J. Phytother. Phytopharm. 17: 684-689.

Westerhuis, J.A., Velzen, E.J.J. van, Hoefsloot, H.C.J., Smilde, A.K., 2009. Multivariate paired data analysis: multilevel PLSDA versus OPLSDA. Metabolomics 6: 119-128.

ABSTRACT IN KOREAN

본 연구에서는 포도나무의 2 가지의 주요한 병인 *Pseudocercospora vitis* 에 의해 발병하는 갈색무늬병과 *Agrobacterium vitis* 에 의해 발생하는 줄기혹병의 병관련 대사산물들의 구명을 위해 GC-MS 와 같은 분석기기를 이용하였고 통계적 검증은 다변량분석을 적용하였다. 갈색무늬병의 시험에서는 총 20 개의 대사산물이 병반과 병반주변부의 조직 사이에 차이가 있는 것으로 확인되었고 대부분이 병반 주변부에서 증가하는 것으로 확인되었다. 줄기혹병에서는 13 개의 대사산물이 반응 유형별로 유의하게 증가함을 확인하였고, 대부분이 줄기혹병 접종 후에 나타났으며, 다른 시기보다 접종 2 일 후 분석한 시료에서 많았다 (8 종). 또한 감수성 그룹(7 종)에서 저항성 그룹(3 종), 중도저항성 그룹(1 종) 보다 많았다. 이는 phytoalexin 인 resveratrol 이 저항성 그룹에서 유의하게 높은 것을 제외하고 대부분의 병관련 대사산물이 gall 의 형성 촉진을 위해서 병원균에 의해 유도될 수 있음을 의미한다. Maltotriose, glucoheptonic acid, tartronic acid, 1-hydroxyanthraquinone, aspartic acid, L-threonine 등 총 6 개의 대사산물이 갈색무늬병 이병엽과 정상엽과의 비교에서 확인되었다. 이들은 이병부 주위에서 광범위하게 일어나는 병과 관련된 대사산물로 판단된다. 줄기혹병에서는 대부분의 여러 대사산물들이 접종(상처) 2 일 후에 감수성그룹(8 종 대사물질)에서 상처 처리구에서는 저항성그룹(4 종 대사물질)에서 유의한 것으로 나타났고, 그 다음은 접종(상처) 7 일 후에 3 종의 대사물질이 병접종의 감수성그룹에서, 6 종의 대사물질이 상처처리의 감수성그룹, 1 종이 상처처리의 중도저항성그룹에서 유의적으로 높게 나타났고, 마지막으로 접종 30 일

후에 3 종의 대사물질이 모두 병접종의 저항성과 중도 저항성그룹에 유의한 것으로 나타났으나 상처처리구에서는 유의적으로 나타난 대사물질이 없었다. 이는 병원균 접종에 대한 반응은 대부분 post-1 시기의 감수성그룹에서 많이 발생하였고, 상처를 치유하는 반응은 감수성보다는 저항성에서 먼저 시작됨을 알 수 있었다. 또한 상처처리 30 일 후에는 상처가 완전히 치유되어 상처에 대한 아무런 반응을 관찰할 수 없었다. 결과를 정리하면 식물의 저항성과 상처치유반응은 상호 연관되어 저항성그룹에서의 상처치유 반응은 병원균 감염에 대한 저항성을 강화한다. 이와 같은 대사산물 분석에 의한 각각의 병에 대한 반응 특성은 포도나무에 발생하는 병의 관리 전략을 발전시키는데 중요한 정보와 새로운 시각을 제공한다.

Supplementary Table 1. Statistical parameters of each compared OPLS-DA models and the result of cross-validation ANOVA(CV-ANOVA).

Stage[a]	Model	$R_2X_{(cum)}$[b]	$Q_2X_{(cum)}$	CV-ANOVA (*p*)[c]	Significance[d]
Pre	SS vs RR	0.694	0.588	0.113	ns
	SS vs SR	0.575	0.218	0.888	ns
	RR vs SR	0.580	0.748	< 0.001	**
Post 1	SS vs RR	0.569	0.620	0.078	ns
	SS vs SR	0.643	0.800	0.007	**
	RR vs SR	0.546	0.721	0.010	*
Post 2	SS vs RR	0.680	0.767	0.016	*
	SS vs SR	0.610	0.521	0.262	ns
	RR vs SR	0.645	0.708	0.009	**
Post 3	SS vs RR	0.620	0.587	0.114	ns
	SS vs SR	0.683	0.281	0.861	ns
	RR vs SR	0.589	0.662	0.030	*

[a]Two days before inoculation (pre), and 2 d (post 1), 7 d (post 2) and 30 d post inoculation (post 3).

[b]R_2X(cum): the cumulative sum of squares(SS) of the entire X explained by all extracted components (Explanation power); Q_2X(cum): the cumulative Q_2 for all the X-variables (PC) and y-variables (PLS) for the extracted components (Prediction power). This parameter was acquired from Simca-P (ver. 12.0).

[c]ANOVA of cross-validated predictive residuals of OPLS analysis.

[d]**; Correlation is significant at $P \leq 0.01$(2-tailed), *; significant at $P \leq 0.01$(2-tailed), ns: not significant.

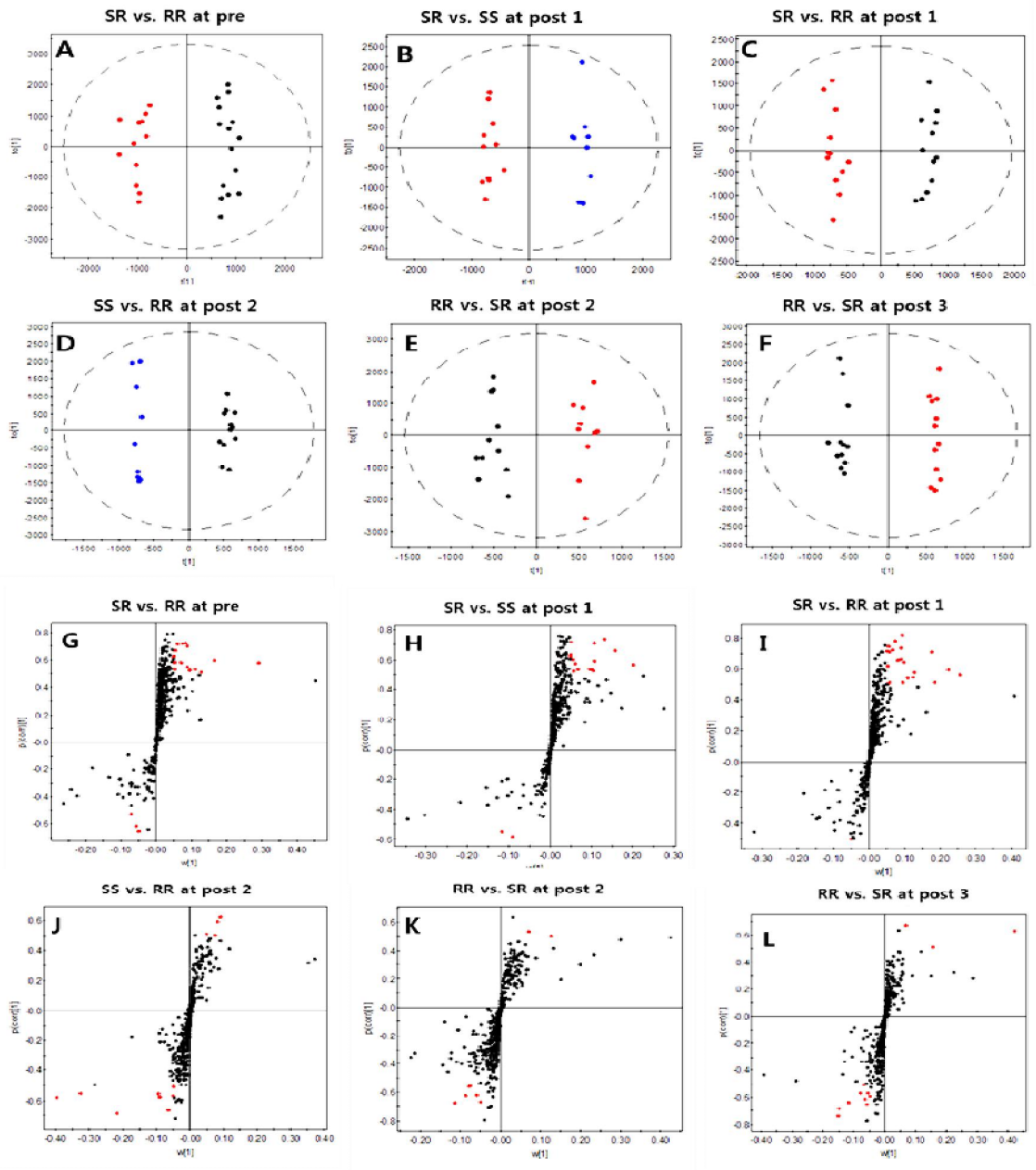

Supplementary Figure 1. OPLS-DA sample scatters plots (A to F) and their metabolite S-Plots (G to L) of different response types (RR; resistant, SR; moderately resistant, SS; susceptible). In scatter plot, Black dots represent RR, red dots SR, and blue dots SS. The short dashed circle is shown Hotelling's T-squared distribution (0.95). In S-plot, metabolites marking red dots are selected by VIP score (>1, PLS-DA) and *p(corr)* value [0.5 < *p(corr),* OPLS-DA]. Collected metabolites are shown in Table 3.